

Plans for  
**TEVATRON RUN IIB**

May 17, 2001

<b>1. INTRODUCTION</b>	<b>5</b>
<b>2. PROJECT STRATEGY, SCOPE &amp; GOAL</b>	<b>5</b>
<b>2.1 Run IIa Expectations</b>	<b>5</b>
<b>2.2 Run IIb Strategy</b>	<b>6</b>
2.2.1 Protons on the antiproton production target.	7
2.2.2 Antiproton collection.	7
2.2.3 Antiproton cooling	8
2.2.4 Antiproton Transport	8
2.2.5 Antiproton tuneshift in the Tevatron	8
<b>2.3 RunIIb Goals</b>	<b>9</b>
<b>3. SUB-PROJECT DESCRIPTIONS</b>	<b>10</b>
<b>3.1 Proton Source</b>	<b>10</b>
3.1.1 Linac	10
3.1.1.1 Ion Source	10
3.1.1.1.1 Motivation.	10
3.1.1.1.2 Program.	10
3.1.1.1.3 Status.	11
3.1.2 Booster	12
3.1.2.1 Ramped Correctors	12
3.1.2.1.1 Scope	12
3.1.2.2 Cogging	13
3.1.2.2.1 Scope	13
3.1.2.2.2 Current status	13
3.1.2.2.3 Future short-term plans or machine studies	14
<b>3.2 Main Injector</b>	<b>15</b>
3.2.1.1 Scope	15
<b>3.3 Anti-Proton Source</b>	<b>21</b>
3.3.1 Target Station	21
3.3.1.1 Solid Lithium Lens	21
3.3.1.1.1 Scope	21
3.3.1.1.2 Status	23
3.3.1.2 Liquid Lithium Lens	25
3.3.1.2.1 Scope	25
3.3.1.2.2 Status	26
3.3.1.3 Beam Sweeping	26
3.3.1.3.1 Scope	26
3.3.1.3.2 Status	27
3.3.2 Debuncher	28
3.3.2.1 Aperture	28
3.3.2.2 Lattice Upgrades	29
3.3.2.2.1 Betatron Coupling Correction	29
➤ Scope	29
➤ Studies	30

3.3.2.2	Resonance Correction	31
➤	Scope	31
➤	Studies	32
3.3.2.2.3	$\gamma_t$ ramp	33
➤	Scope	33
➤	Studies	34
3.3.3	Accumulator	35
3.3.3.1	Accumulator Cooling for Run IIb	35
3.3.3.2	Description of stochastic stacking	35
<b>3.4</b>	<b>Recycler</b>	<b>41</b>
3.4.1	Electron Cooling	41
3.4.1.1	Background	41
3.4.1.2	Project Scope	42
<b>3.5</b>	<b>Rapid Antiproton Transfers</b>	<b>44</b>
3.5.1	AP2 Line	45
3.5.2	AP5 Line	46
3.5.2.1	Design	46
3.5.2.2	Civil	46
3.5.2.3	Technical Components	46
<b>3.6</b>	<b>Tevatron</b>	<b>47</b>
3.6.1	Longitudinal Dynamics	47
3.6.1.1	Scope of Project	47
3.6.1.2	Current Status	47
3.6.1.3	Future Plans	50
3.6.2	Beam-Beam Tune Shift Compensation	51
3.6.2.1	Scope	51
3.6.2.2	Status	52
3.6.2.3	Further Studies and Plans	53
<b>4.</b>	<b>RESOURCES, COST, SCHEDULE</b>	<b>55</b>
4.1	Project Goals	55
4.2	Project Costs by Sub-Project	57
4.3	Project Effort	60
4.4	Project Materials and Service Costs	62
4.5	Project Total Cost	63
4.6	Project Schedule	64
<b>5.</b>	<b>SUMMARY</b>	<b>65</b>
<b>6.</b>	<b>REFERENCES</b>	<b>65</b>



## 1. Introduction

It is recognized that an experimental program, in the course of which greater than  $15 \text{ fb}^{-1}$  of integrated luminosity is delivered by the Tevatron complex to each of the two collider experiments, CDF and D0, has considerable discovery potential [1]. Achieving this integrated luminosity requires an increase in the instantaneous luminosity of a factor of 2-3 beyond that anticipated during Run IIa (the current run). The robustness of the physics program would be enhanced if more integrated luminosity could be achieved. The window of opportunity is bounded in time by the start of operation of the Large Hadron Collider for physics, which is anticipated in 2006 or 2007.

Considerable work was done to examine the potential of the Tevatron complex to achieve such a goal. An extensive report [2] was prepared by April 1997 but not completed nor published. The plan described in this report does not include all the possibilities suggested in that report.

In this document we concentrate on justifying the approach currently proposed, and describe a plan of execution, which we feel is responsive to the imperatives of the physics. In Chapter 2, we outline the overall strategy and scope. The components of the project are distributed throughout the accelerator complex. The priorities and schedules have been developed by balancing the difficulty and cost of each sub-component versus its potential to enhance the performance of the overall complex as a function of time. In Chapter 3, we describe the scope and current status of each of the sub-projects. In Chapter 4, we provide a summary of the needed resources, the cost and schedule. Where a subproject is sufficiently mature, input has been taken from that sub-project. Where not, a top-down assessment has been made. Finally in Chapter 5, we summarize.

We hope that the structure of this document will accommodate expansion into a more complete Technical Design Report in due course.

## 2. Project Strategy, Scope & Goal

### 2.1 Run IIa Expectations

The Run IIa scenario, which we assume [3], is encapsulated in Table 2-1. Initial operation will be with 36 proton bunches and 36 antiproton bunches in three trains of twelve bunches each separated by 396 ns. The gaps between the trains provide for abort of the two beams. The Recycler Ring will be operational and the mechanism, which enables both storage of antiprotons from the source and cooling of recovered antiprotons from the Tevatron, will be implemented. The possibility of luminosity leveling will also exist.

As the instantaneous luminosity approaches  $1 \times 10^{32} \text{ cm}^{-2} \text{ sec}^{-1}$ , a change will be made to operate with bunch spacings of 132 ns, and up to 140 proton bunches and 105 antiproton bunches loaded in the machine. This prevents the mean number of interactions in each bunch crossing rising above three. (As the number of interactions per crossing rises, the occupancy of the detectors increases, and they become more difficult to operate successfully.) The time structure of the bunch trains is somewhat different than that for 36x36 operation but gaps to permit beam abortion will need to be retained. With this bunch spacing, satellite extra bunch crossings on either side of the B0 and D0 intersection points can only be avoided by introducing a crossing angle of 136  $\mu$ radians between the beams. The number of protons per bunch and the number of antiprotons per bunch are  $2.7 \times 10^{11}$  and  $4.0 \times 10^{10}$  respectively. With this configuration the peak instantaneous luminosity is expected to reach  $2 \times 10^{32} \text{ cm}^{-2} \text{ sec}^{-1}$ .

**Table 2-1 Machine Parameters for Run IIA and RunIIB of the Tevatron.**

Parameter	Run IIA 140x105	Run IIB 140x105	Units
Protons/bunch	$2.7 \times 10^{11}$	$2.7 \times 10^{11}$	
Antiprotons/bunch	<b><math>4.0 \times 10^{10}</math></b>	<b><math>1.0 \times 10^{11}</math></b>	
Req'd Pbar Production Rate	<b>21</b>	<b>52</b>	$10^{10}/\text{hr}$
Proton emittance (95%, norm)	$20\pi$	$20\pi$	mm-mrad
Antiproton emittance (95%, norm)	$15\pi$	$15\pi$	mm-mrad
Energy	978	978	GeV
No. of Pbar Bunches	103	103	
Bunch length (rms)	0.37	0.37	m
Bunch Spacing	132	132	nsec
<b>Typical Luminosity</b>	<b><math>2.1 \times 10^{32}</math></b>	<b><math>5.2 \times 10^{32}</math></b>	<b><math>\text{cm}^{-2} \text{ sec}^{-1}</math></b>
Interactions per crossing	1.9	4.8	
<b>Integrated Luminosity</b>	<b>42</b>	<b>105</b>	<b><math>\text{pb}^{-1}/\text{week}</math></b>

## 2.2 Run IIB Strategy

With the machine parameters foreseen for RunIIa, it is still expected that the primary limitation on the luminosity will be imposed by the total number of antiprotons available. The standard expression for the luminosity is

$$L = \frac{3\gamma_r f_0}{\beta^*} (BN_p) \left( \frac{N_p}{\epsilon_p} \right) \frac{F(\beta^*, \theta_x, \theta_y, \epsilon_p, \epsilon_{\bar{p}}, \sigma_z)}{(1 + \epsilon_{\bar{p}}/\epsilon_p)},$$

which clearly manifests the dependence on this parameter. The basic strategy is therefore to try and increase the total number of antiprotons available for collisions. Some components of the plan address actual increases in numbers of protons on target and in numbers of antiprotons produced. Other components may have no associated numerical increase but are just as important because their failure to operate with 100% efficiency can negate the gains in other areas.

### **2.2.1 Protons on the antiproton production target.**

Studies [4] have shown that in order to achieve very high performance of the proton source (Linac and Booster) there are many issues that need to be addressed. In turn this results in a rather expensive project to make big improvements in the intensity of protons out of the Main Injector. We therefore have limited ourselves to two subprojects. Historically the intensity out of the Booster, over a range of conditions has been proportional to the intensity of ions out of the H source. Therefore, we have retained a modest source-improvement R&D program. This will be accompanied by quantitative measurements of the relationship between Source performance and Booster performance

At the present time, the Main Injector is filled by injection of six successive Booster batches. When operating for both NUMI and anti-proton production, and given the cycle times of the machines, the ability to overlay further booster batches would lead to an increase in protons on the antiproton production target. This could be achieved using slip-stacking, a technique which has been demonstrated on other machines including the Fermilab Main Ring. A program to implement this is in the early stages. In order for this to work effectively it is expected that some beam-loading compensation equipment will need to be provided in the Main Injector. It is expected that the improvements would lead to an increase by a factor of 1.8 in the number of protons on target per unit time.

### **2.2.2 Antiproton collection.**

The antiprotons are produced, by impinging the beam, extracted from the Main Injector, on a nickel target. The phase space of the resulting antiprotons is controlled by the physics of the production process. A pulsed Lithium Lens is used to focus the antiprotons into the AP2 beamline. The Lithium lenses exhibit a finite lifetime, which is lower for higher currents. Although the understanding of lens failure is not complete, the current design has certain identifiable weaknesses. Two approaches are being pursued. On the one hand, a new solid-Lithium lens design is well advanced. On the other, an R&D project, involving the use of liquid Lithium, is underway in collaboration with the Budker Institute, Novosibirsk. Since the handling of liquid Lithium is very difficult, the liquid lens is treated as more speculative than the solid lens work.

This work on lens construction is complemented by an attempt to better understand the physics of the entire production and collection process. It is thought that a factor of 1.5 in the antiproton yield might be available with success in both areas.

After production, the antiprotons are transported to the 8 GeV Debuncher machine through the AP2 beamline. Studies are underway to understand the limitations in the aperture of this line, and also the aperture of the Debuncher machine itself, with a view to improving the performance of each. The potential increases in these apertures are of the order of a factor 1.5.

### **2.2.3 Antiproton cooling**

The antiprotons need to be cooled in the Debuncher, Accumulator, and Recycler Ring. In the first two, the cooling is only stochastic. In order to improve the system to accommodate the increased numbers of antiprotons the cooling bandwidth in the Debuncher should be addressed along with several of the aspects of the multifaceted Accumulator cooling. This includes the bandwidth of the core cooling system.

At present, stochastic cooling is installed in the Recycler Ring. A major R&D program has been underway for some years to develop an electron cooling capability. A major installation is in place in one of the fixed target experimental halls. This setup, complete with Pelletron, has recently achieved beam recirculation.

### **2.2.4 Antiproton Transport**

When the antiproton production rate is high, and the cooling in the accumulator is efficient, it is important to have a ready repository for the cooled antiprotons. That repository must be the Recycler Ring. In the present configuration, the antiprotons are transferred from Accumulator to Recycler Ring along a beamline, which is multi purpose, and must operate both at 8 GeV and at 150 GeV. This line has proved to be difficult to tune and operate. In the new regime, tuning and transfer must take place within minutes. Studies, of the optics of this complex line, are underway with a view to modifications, which show some promise on paper. If unsuccessful a dedicated line would be needed. Dubbed the AP5 line, such a possibility is accommodated in the project plan.

### **2.2.5 Antiproton tuneshift in the Tevatron**

In the Tevatron, the antiproton bunches suffer a tuneshift due to their interactions with the more intense proton bunches. In multibunch operation, the tuneshifts vary from antiproton bunch to antiproton bunch, leading to an effective spread in tune. An electron lens, consisting of a short, low energy, electron beam propagating along the axis of a solenoidal field, can induce a tuneshift on the antiproton bunches, which has the opposite sign to that, which they experience, from the protons. With appropriate choice of parameters two such lenses could provide effective beam-beam tuneshift compensation. An R&D program has resulted in the construction and, recently, the successful testing of a single such device. If results continue to be positive the use of such devices could lead to a longer luminosity lifetime in the Tevatron and hence to a large integrated luminosity.

### **2.3 RunIIb Goals**

In the above, we have discussed ways to increase the protons on target per unit time by a factor of 1.8, a way in which the antiproton yield can be improved by a factor 1.5, and one where the antiproton collection can be improved by another factor 1.5. Together with the improvements to the complex to better handle the increased production rates of antiprotons and to transport them to collision with the appropriate phase space parameters, an increase, by a factor of 2-3, in luminosity, should be achievable. These improvements are encapsulated in the parameter list for Run IIb shown in Table I.

We note that no credit has been taken for potential improvements in the Linac, nor as a result of the use of the beam-beam tuneshift compensation in the Tevatron. However, it is worth reiterating that a prerequisite for the gains claimed above is the operation of the Recycler Ring.

### 3. Sub-Project Descriptions

#### 3.1 Proton Source

##### 3.1.1 Linac

###### 3.1.1.1 Ion Source

###### 3.1.1.1.1 Motivation.

The Linac presently delivers a 400-MeV  $H^-$  beam to the Booster with an intensity of 45-55 mA. The typical normalized emittance is  $\sim 7-8 \pi$  mm mrad and the momentum spread is  $\sim 0.25\%$  (both for 90% of the beam). It has been shown with protons that an intensity of  $\sim 80$  mA can be transmitted through both the low- and high-energy linacs without significant changes in the RF systems and little increase in the losses. This is about the maximum for the Linac without major modifications in the RF systems or injection to the Linac. Obtaining 80 mA from the Linac requires 115+ mA from the ion source using the Cockcroft-Walton since only 70% of the continuous source beam can be effectively bunched and captured into linac buckets at injection. Except for the 30% loss at injection due to RF capture the other beam losses are only a few percent. At injection there is also a significant emittance growth in the beam due to errors in the earliest part of the Linac. Therefore, the motivation for ion source R&D is to increase the source intensity to increase the Linac output; while also increasing the source brightness (lower the beam emittance) to decrease the Linac losses and radiation levels as the intensity and repetition rates increase.

###### 3.1.1.1.2 Program.

An  $H^-$  source R&D program is proposed below. This effort will involve: (1) work on improvements to the present magnetron source (planotron in Russian) to increase the  $H^-$  beam intensity and brightness; and (2) work on a semi-planotron source (basically half of a magnetron), which could replace the magnetron source and produce a noiseless beam of 110+ mA with high brightness.

- Improvement of the magnetron:.

The emittance (brightness) of the present magnetron may be improved by optimizing the discharge geometry, gas injection, extraction and plasma over-neutralization. The goal is to attain a reliable 85-100 mA of  $H^-$  with an emittance of  $0.5 \pi$  mm-mrad (90%, normalized), which is a factor of two smaller than the present 750-keV beam emittance.

- Development of a noiseless semi-planotron.

Here, the goal is to obtain 110+ mA of  $H^-$  beam at 750 keV with an emittance of  $0.7 \pi$  mm-mrad (90%, normalized). This source is small so it could be adapted for installation in the Cockcroft-Walton as a replacement to the magnetron.

This program represents a first step towards improving the Linac beam. It is a fairly short program (1-2 years) and requires modest investment (a new hire plus \$60k M&S funds). If successful and the Booster responds favorably to the beam, this effort may have a small impact on the present Linac and Booster performance. This is because these new sources can be mounted on the Cockcroft-Walton and provide an  $H^-$  beam with higher intensity and better quality (i.e., a brighter beam). Decreased beam size in the Linac should decrease the beam loss and radiation allowing higher intensity and repetition.

It is recognized that for a significant future improvement of the  $H^-$  beam quality for the existing Linac and future Proton Driver it would be necessary to develop an  $H^-$  source giving a very high brightness, such as a Penning geometry Surface-Plasma Source, known as a Dudnikov type  $H^-$  source, or other source that could be fitted to an RFQ accelerator, which would replace in some manner the first two MeV of Linac tank one.

#### 3.1.1.1.3 Status.

Active work on the magnetron  $H^-$  source has not been done for sometime. Still the test bench and most of the parts and power supplies are in the ion source lab. Restarting this effort is not too difficult. An Associate Scientist has recently been hired into the Linac Group for this purpose. He is to begin July 1. It appears that some magnetron studies will be underway within a few months. In addition to this person, Vadim Dudnikov and Chuck Schmidt will give some assistance to this effort.

Some work on the semi-planatron has been done recently on the test stand to develop a low-intensity high-brightness DC beam for the electron cooling program. This would need considerably more work before it could replace the operating source.

Basic steps for beginning this program are:

1. Once a new group is formed, begin reestablishing the ion source test stand and begin operation of a standard Fermilab magnetron source.
2. Reinstallation of an emittance scanner, some beam diagnostics and computer acquisition system.
3. Begin studies on the source to understand present operation. An early goal is the characterization of an existing magnetron source beam: emittance scanning for optimal operation condition.

4. Consider source modifications and improvements.
5. An optimization of the discharge electrodes, gas pulsing system, and extraction system of the magnetron. An optimization of the space-charge neutralization with a plasma source. Test operation of the discharge electrodes, gas pulsing system, and extraction. Test long term operation.
6. Move on to the development of a semi-planatron surface plasma source.

### **3.1.2 Booster**

#### *3.1.2.1 Ramped Correctors*

##### 3.1.2.1.1 Scope

Beam loss control at high intensity in the Booster is essential to providing the protons required for Run IIB operation. At issue are both protons available per pulse and radiation concerns. The greatest number of particles lost in the Booster are lost during the first 5 milliseconds of the machine cycle. The Booster currently has DC powered dipole corrector magnets that are used to adjust the low energy orbit to maximize beam acceptance. As the beam energy increases during the acceleration cycle, the beam orbit decays in an uncontrolled manner to a high field orbit determined almost entirely by the gradient magnets and their precise locations.

The goal of the ramped corrector project is install the hardware and software upgrades required to permit individual time-varying control of the corrector magnet currents in order to control the beam orbit to a higher energy than currently possible. Ramp generator cards provided by the Beams Division and RMS over-current protection circuitry provided by the Proton Source Department are required. It is yet to be determined whether upgrades to the corrector magnet power system are necessary to achieve useful results. The voltage rating of the present system limits the available  $di/dt$ . Significant software effort will be required to provide a useful operator interface to the ramp control system and to perform the required background orbit correction computations.

##### ➤ Current status

Currently, ramp generator card hardware is being procured and fabricated by the Beams Division Controls Department. The RMS over-current protection circuitry and necessary modifications to the corrector power supply control chassis' are being prototyped within the Proton Source Department. Software activity has not yet begun.

➤ Future short-term plans or machine studies

Plans are to implement ramp controls on one suitable set of three or four corrector magnets to test hardware designs and to provide a platform on which software implementation can begin and be tested. This will be in place in early summer 2001. Most of the beam studies required for commissioning the ramped corrector system can be accomplished on Booster studies cycles available in the accelerator timeline without interference with Main Injector or other machine operations.

### 3.1.2.2 Cogging

#### 3.1.2.2.1 Scope

Control of high energy beam loss in the Booster is essential to providing the protons required for Run IIB operation. Historically, the Booster has operated with beam bunches in all 84 possible RF buckets around the machine circumference. The Booster extraction kicker magnet rise-time is slower than the time between passage of successive bunches. This mode of operation resulted in the loss of two of the 84 bunches at extraction time as the kicker swept the 8 GeV beam across the extraction septum. This is not acceptable at the high intensities and high average beam pulse repetition rates of Run IIB due to the resulting prompt radiation, component activation, and potential component radiation damage.

Recently operation has been with a short notch or gap created in the 400 MeV Booster beam shortly after injection. Synchronizing the extraction kicker to this notch greatly reduces extraction losses at 8 GeV. This mode of operation is feasible for any Main Injector cycles requiring injection of only one Booster beam batch. Multi-batch injection cycles, e.g. Main Injector slip stacking, do not allow flexibility to the Booster to define the time of transfer. Batches following the first in each Main Injector cycle must be placed in the Main Injector at a precise time and location relative to the previous injected batches. In this mode, the Booster must actively cog the Booster beam notch during the acceleration cycle to synchronize with the Main Injector controlled transfer time.

This cogging project provides the timing and low level RF control hardware and software to create and actively cog beam during Booster acceleration to synchronize with the extraction kickers at the end of the cycle.

#### 3.1.2.2.2 Current status

This project is currently at a "proof of principle" stage. It has been demonstrated that a kicker gap can be created in the 400MeV beam in Booster, tracked throughout the acceleration cycle, and roughly be controlled to synchronize with the extraction timing. The systems tested to date have been mostly successful, but somewhat deficient in achieved

accuracy and rather "unkind" to beam in the process. A kinder, gentler scheme must be created. To make the system operational, a "smarter" control algorithm must be developed, implemented, and proven.

#### 3.1.2.2.3 Future short-term plans or machine studies

This project can be accomplished using only parasitic beam studies cycles without interference to other operations. Progress is currently manpower limited.

## 3.2 Main Injector

### 3.2.1.1 Scope

Slip stacking is a process that increases the overall intensity of a short batch of beam in a circular accelerator through momentum painting. One batch of beam is injected into the accelerator, and the next batch is injected slightly off momentum from the first batch. Since the two batches have different velocities, they will eventually interfere with each other, or one batch will “slip” relative to the first batch. Once the two batches are aligned with each other, a single RF bucket large enough to contain the two batches is snapped on, producing a single batch with twice the charge of an injected batch. See Figure 3-1.

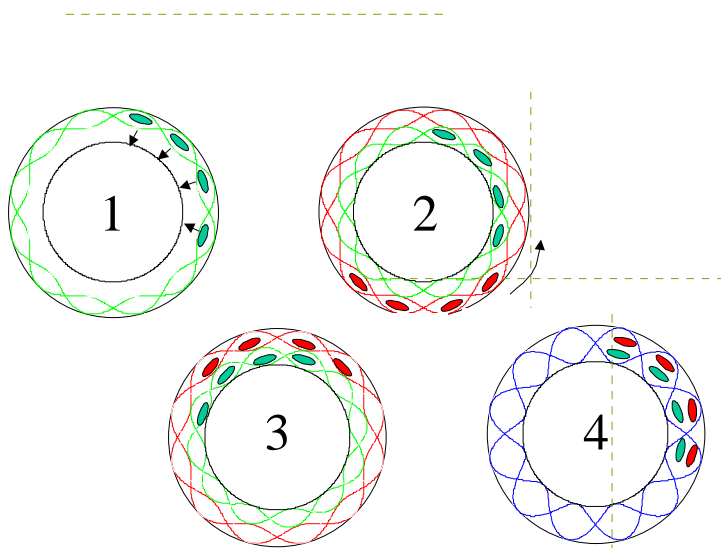


**Figure 3-1** Slip Stacking Mechanics. Item 1 shows the initial batch injection and the deceleration process. Item 2 shows the injection of the 2<sup>nd</sup> batch. Item 3 shows the two batches slipping relative to each other. Item 4 shows alignment and capture.

This technique is very useful when the injecting accelerator has reached its short batch intensity limit, has a short cycle time compared to the downstream accelerator, and the longitudinal emittance is small compared to the acceptance of the downstream accelerator. The Fermilab Booster has reached an intensity limit due to space charge at injection, it has a cycle time of 66 ms, and the final extracted beam has about a 0.5% momentum spread. The main injector has

about a 1.5 s cycle time, and a momentum acceptance of about 1.5%. This makes the main injector a very good candidate for the slip stacking process.

The main impetus for commissioning slip stacking in the Fermilab main injector is to increase the total flux in the antiproton source. The antiproton source debuncher has the same energy and circumference as the booster. One booster batch will fill the debuncher with antiprotons. Obviously, if slip stacking can double the intensity of a single booster batch, then double the amount of protons hit the antiproton production target. As long as the total bunch length of the bunch on target is within the momentum acceptance of the debuncher bunch rotation and cooling system, the higher intensity will translate directly to more antiprotons.

Circulation of multiple batches with different momenta requires separate accelerating voltages, each synched to a different batch. Each batch's RF voltage will affect other batches, and this limits the minimum frequency separation between batches. The minimum frequency separation is a function of a single batch bucket size, which is a function of the total RF voltage at a given batch frequency. The amount of momentum aperture used by the slipping process is proportional to the amount of frequency separation, making a small frequency separation desirable. However, small frequency separations imply very low RF voltages to keep the different batch buckets from interfering destructively, and this may lead to beam loading limitations.

#### ➤ Low Intensity

The first aspect of the project involves studying the slip stacking process at low intensity. Slip stacking at low intensity was already achieved in the main ring and should be straightforward to achieve in the main injector. In the main ring scenario, the first batch was injected on to the outside orbit. The injection field of the main ring was adjusted to allow a close match between the nominal and slip stacking injection frequencies. The first batch was then decelerated to the inside orbit, and the second batch was injected on the outside orbit behind the first batch. The second batch caught up with the first batch, and when the two batches were aligned, the RF frequency was snapped to the frequency of the central orbit, and the RF amplitude was snapped high enough to contain both batches. Both the low level RF and high level RF control systems must be modified to enable slip stacking. Also, bunch rotation in the booster must be used to match to the low voltage buckets.

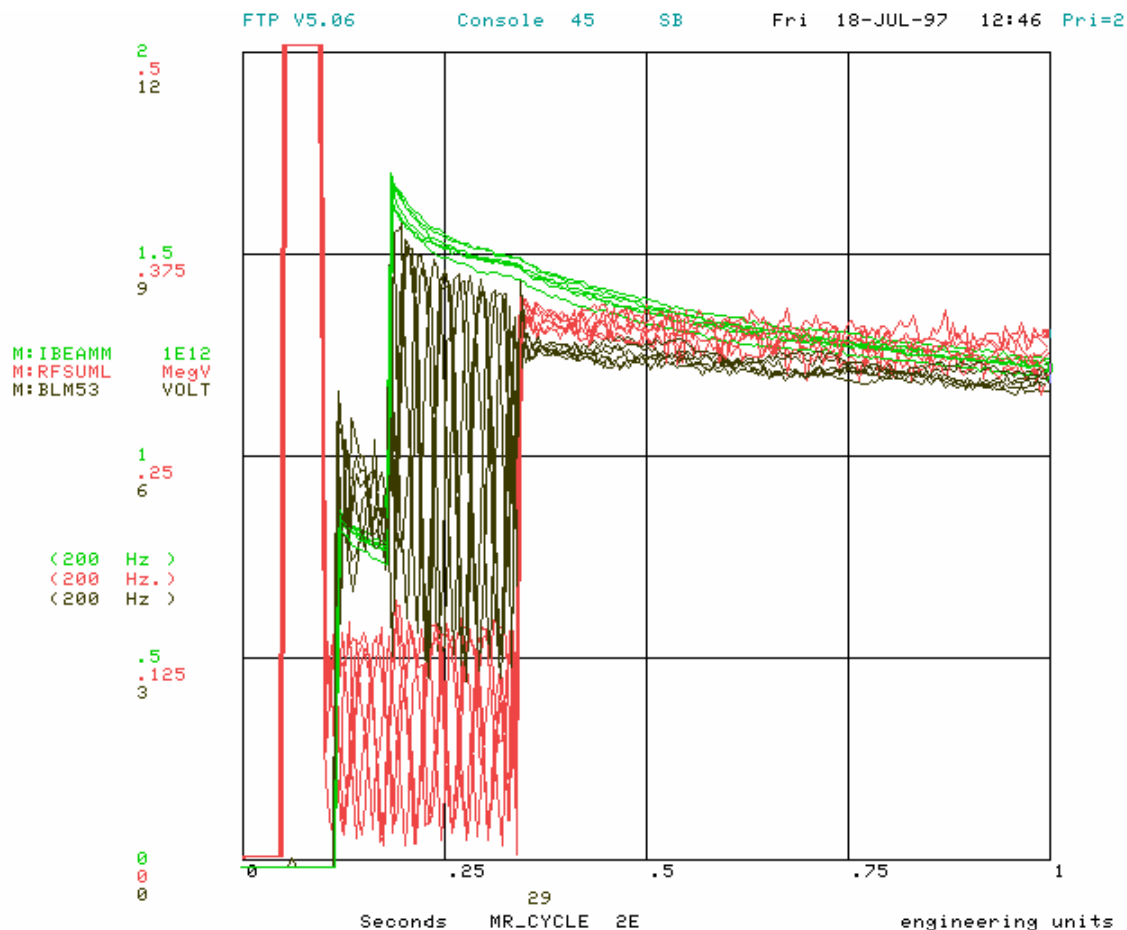


**Figure 3-2** Main Ring Slip Stacking Experiment. Results from slip stacking approximately  $7.5e11$  proton batches. Green – Beam Intensity ( $0.5e12/\text{div}$ ). Red – RF Sum ( $125\text{kV}/\text{div}$ ). Black – 53MHz component of beam from current monitor (relative scale). Note beating of RF Sum and 53MHz component during slipping.

The low level RF system must provide all of the necessary beam synchronous RF signals for the different batches. It must provide multiple, precise, yet controllable frequency programs. During the low intensity studies, the low level RF system will be used to determine the optimum frequency separation between slipping bunches. Therefore, the frequency separation must be a user-defined parameter. Also, the system must be able to recognize when the batches are aligned and snap the frequency outputs to the proper synchronous frequency for the central orbit of the accelerator. This may be done internal to the low level RF system, or it may be done with a precise external trigger.

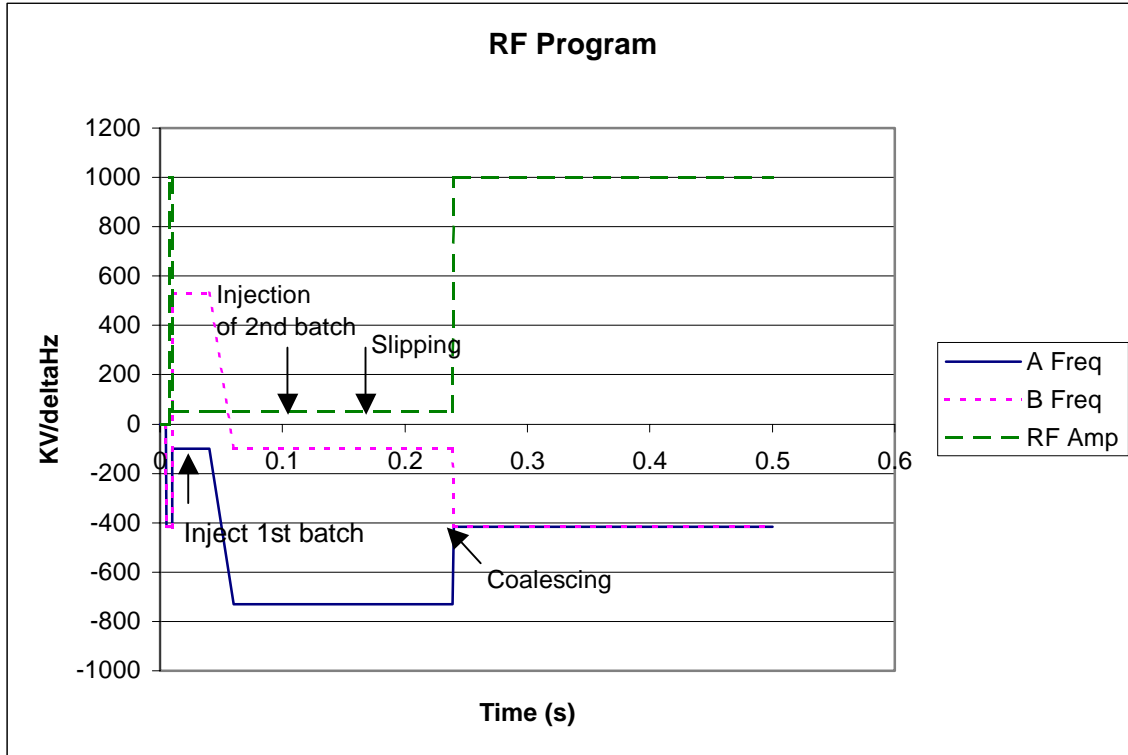


**Figure 3-3 Sample Frequency/Voltage Program. Before beam, all cavities are on and tuned to central orbit frequency. Tuning errors are sampled and held, and voltage is reduced to 50kV / batch. First batch is injected close to nominal orbit and decelerated. Second batch is then injected and two batches slip until aligned about 130ms later. Offset frequencies are snapped to new central orbit, and cavities are set to the higher voltage.**

The low level RF system must also provide the necessary synchronization ( see Section 3.1.2.2 )between the Booster and the Main Injector. The Booster must always phase lock to the Main Injector injection orbit for each transfer, which implies that it cannot use the RF synchronous with a batch that has been accelerated after injection. The low level RF system must also provide markers that track the revolutions of each batch. These markers will be used to determine the proper injection location in main injector from the booster, and they might be used to determine when all of the batches are aligned.

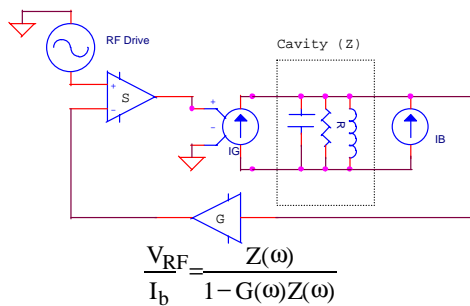


**Figure 3-4 Direct RF Feedback.**  
*Impedance seen by the beam is reduced by the loop gain.*

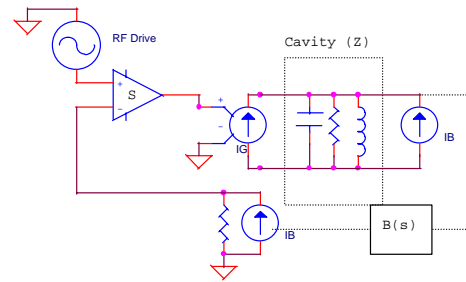


**Figure 3-5 Feedforward.** *A signal from the beam is fed into the drive.*

The high level RF system must provide the low voltages necessary to maintain sufficient bucket separation between different batches. For most low voltage processes in the main injector, the cavities are run at moderately high voltages, but paraphased to supply a very small, net RF voltage. The fanout distribution used to provide each set of cavities with the proper paraphase angle is used to provide the different batch frequencies for slip stacking. We cannot use the same system for paraphasing during slip stacking cycles. Optimally, the cavities could be configured so that they could run at the low voltages necessary without the aid of paraphase. This involves using fundamental mode beam loading compensation to regulate the cavity voltage, and it involves disabling/enabling high level feedback loops in a smooth fashion. If this proves to be too costly and impractical, a new fanout distribution system will be installed. This system will provide a pair of paraphased outputs for each batch frequency to be distributed to the cavities.

Once the low level RF and high level RF systems are in place, low intensity slip stacking studies will begin. These studies will determine the optimal frequency separation between batches while they are slipping. They will determine the optimal RF voltage and bucket size, before and after coalescing. They will also determine the slip stacking intensity limit with the current RF hardware. The intensity limit will be analyzed to determine its cause and what hardware modifications are necessary to overcome the limit.

### ➤ Beam Loading/High Intensity

One of the most obvious mechanisms limiting slip stacking intensity is beam induced voltage. The voltage generated by the beam will be more than a factor of ten times the RF voltage for typical stacking intensities during slip stacking. This voltage will destroy the buckets used to contain the slipping batches and render slip stacking ineffective unless a means to compensate the voltage is devised. Two beam loading compensation systems will be commissioned during the low intensity slip stacking studies. One system uses cavity feedback to reduce the impedance of the cavity at its fundamental resonance as seen by the beam. The system can reduce the beam induced voltage by a factor of twenty, and this enables the system to run at very low voltages with reduced interference from the beam. The second system uses a beam wall current monitor and a delay to provide the cavity drive with a beam current signal that it can use to preempt beam current in the cavity. This technique is referred to as feed-forward beam loading compensation. Commissioning these systems should increase the intensity limit, and although they may not be enough to reach the intensity specifications, they should provide enough information to specify a more flexible beam loading compensation system.

#### ○ Particle Tracking

Particle tracking simulations are used to analyze slip stacking limitations. These simulations will be used to generate the RF specifications necessary for slip stacking. The software used for the simulations has already been modified to allow for multiple batches at multiple energies. Work is continuing on the simulation software to include beam-induced voltages in the cavities. The purpose of the low intensity studies is to verify the accuracy of the simulations under different operating conditions. Most importantly, the simulations should predict slip stacking efficiency with different beam loading and beam loading compensation parameters. Once the simulations predict the low intensity process with reasonable accuracy, the simulation will be used to extrapolate the effectiveness of the process at high intensity. The beam loading compensation specifications will be determined from the results.

### ➤ Future Work

Upon completion of the low intensity studies, work will begin on the modifications necessary to make slip stacking operate at normal stacking intensities. This may involve a digital cavity feedback system that provides a factor of 100 reduction in beam induced voltage. Another modification may involve better power amplifiers for the cavities themselves in order to increase the total available RF voltage and allow for the ability to capture batches separated by larger frequencies. Work will be complete when the main injector provides 75% more beam on target during stacking within the momentum aperture of the antiproton source.

### **3.3 Anti-Proton Source**

#### **3.3.1 Target Station**

##### *3.3.1.1 Solid Lithium Lens*

Efforts to create a reliable, high gradient (greater than 10 Tesla surface field), solid lithium conductor, collection lens for Run IIb are being concentrated in three areas. First, the current collection lens design is being investigated to discover the nature of past failures and any predictable shortcomings of the structural design. Second, design and analysis of new lens design possibilities are being conducted with the end goal of producing and testing prototype high gradient lenses. Finally, since there are indications that the lithium pre-load pressure is important to lens survival, research and development of an improved lens filling process is underway.

##### **3.3.1.1.1 Scope**

###### ➤ Current Lens Design Investigation

The existing collection lens design is being investigated in order to identify areas of improvement for future lens development. Activity is occurring on two fronts: autopsy of failed lenses and finite element analysis (FEA) of the actual design.

###### ○ Autopsy of Failed Lenses

In the past, autopsy of failed lenses has been avoided due to the hazardous nature of radioactive lithium. However, with careful planning and controls in place (and since failed lenses have had appreciable time to decay), it is now thought to be safely achievable. Autopsy of the lenses will be performed by melting and removing the lithium conductor core, and then rinsing with water, in order to react away any residual lithium. The work will be performed in an inert atmosphere with byproducts carefully collected and measured. After the emptied lens is disassembled, the various lens components may be visually inspected to identify locations and mechanisms of failure. Since failures have primarily consisted of breaches of the titanium cooling jacket (septum) allowing lithium into the cooling water medium, it is hoped that inspection might indicate areas of the septum that require improvement.

###### ○ Finite Element Analysis of Current Lens Design

FEA of the current lens design is being conducted to provide a complete visualization of the structural stresses in lens components during a pulse. The current level of FEA technology enables geometrical details and cyclic loading to be modeled that have not been included in previous analyses. The FEA of the current lens design starts with a thermal diffusion simulation of the current pulse, includes thermal and structural stress effects, and results in stress and deflection of lens components at time points of interest. All of this is done within the ANSYS FEA package. A Fermilab PPD ANSYS expert, Z. Tang, is developing this analysis method. It is hoped that results will indicate any weak points of the current lens design that can be correlated with actual lens failure autopsy results. This will greatly aid in the future design of high gradient solid lenses.

### ➤ New High Gradient Solid Lens Design

Design efforts for a new high gradient lens are focussing on four areas. First, a method of simulating how lens geometry changes (radius, length, end regions, etc.) affect anti-proton yield is being developed. Second, the same FEA tools described above will be utilized to evaluate new lens designs. Third, a new joining technology (namely diffusion bonding) is being investigated for high gradient lens application. Fourth, the results of the above three areas are being applied in a prototype program that will allow real-world testing of lens design improvements.

#### ○ Lens/Beam Physics Modeling

The existing design of the solid collection lens is similar to that originally conceived in the early 1980s. The lens was designed to operate with a surface field of 1000 Tesla/meter, but rather early in the target station history, it was determined that extended operation for millions of pulses is not possible above about 750 Tesla/meter. As a consequence, the collection efficiency has been less than desirable. Pbar collection is a complex, multivariable problem. Late in the 1990s, A program called MCLENS based upon the shielding code CASIM was written to model the operation of the lens. Work with the MCLENS code has suggested that a smaller diameter lens with the same 1000 Tesla/meter surface field would provide superior pbar collection to that offered by the existing lens design at its limited operating gradient. One perceived shortcoming in the MCLENS program is that the magnetic field is modeled as an infinite cylinder and does not consider end effects. This results in the overestimation of both the actual collection lens length and efficiency.

A new collection lens modeling effort based upon the MARS code has been undertaken. In the MARS version of the collection lens model, non-linear, magnetic field end effects are considered. As with MCLENS, multiple scattering and other beam interaction effects are treated. Experimental data will be compared with the MARS model to determine if the model accurately predicts behavior of the existing collection lens. Once the model has been shown to emulate operation of the existing design, the parameters of the collection lens such as length, diameter, and field will be altered in conjunction with the engineering design. The use of this improved code may provide confidence in conclusions provided by the MCLENS code. Ultimately, a new collection lens design must meet engineering/structural requirements and show improved beam physics performance as measured by pbar production efficiency (pbars per proton on target.)

#### ○ FEA of New Lens Designs

Using the same FEA tools developed by Z. Tang of PPD to analyze the current lens design, design improvements for the new high gradient lens will be analyzed. Effects of various materials for different components, geometrical changes, cooling parameter changes on component stresses will be investigated. As previously described, the model will simulate several cycles of loading (several hundred pulses) to achieve quasi-static status. Then stress results will be looked at from a fatigue perspective to evaluate proposed design changes.

#### ○ Diffusion Bonded Septum Joints

The current method for joining individual septum components is electron beam welding. Although this method can be highly successful, it has its drawbacks in terms of fatigue, weld to weld consistency, and costs. Another method of joining (diffusion bonding) has been identified

and will be investigated for applicability to septum construction. This new method of joining uses high temperature and moderate pressure to achieve complete bonding (crystal growth across joint) with more uniform microstructure, less residual stress, and for less cost than electron beam welding. Use of diffusion bonding, however, is untried for this application and requires major geometrical changes for maximum benefit. These geometrical changes can be included in the FEA mentioned earlier. Fatigue testing of sample diffusion bonded joints is also planned in order to determine and compare endurance limits of the joining method.

- Prototype Program

Design improvements indicated by all the above, are planned to be tested in a series of prototype high gradient lenses. The prototypes will be constructed on an aggressive schedule in order to meet Run IIb needs. The prototypes will allow us to test pulse the new designs in a real-world operating environment. It is expected that at least two prototypes will be required before succeeding at the goal of a robust (10 million + pulses), high gradient (10+ Tesla surface field) solid collection lens.

- Lens Filling Research and Development

Past experience and preliminary simulation results have strongly indicated that lithium pre-load pressure is linked to long term success of a solid lithium collection lens. Pre-load pressure is necessary to oppose the magnetic pinching effect during a current pulse and keep the lithium conductor material from separating from the septum wall. Currently this pressure is provided during the initial fill of the lens with lithium. Unfortunately, because of the difficulty with volume contractions of the lithium and problems with instrumentation of the lens itself, confidence that proper pre-load pressure has been attained is not high. Research and development is currently underway to improve the fill process in terms of equipment, instrumentation, and data acquisition so that future fills of both current lenses and prototype lenses will be successful. In addition research and testing is planned to explore the possibility of adjusting the pre-load after the actual fill using, as of yet, un-designed mechanisms.

### 3.3.1.1.2 Status

- Current Lens Design Investigation

- Autopsy of Failed Lenses

Five solid lenses, which have failed in service, are to be disassembled to determine the failure modes. The removal of lithium from the lenses occurs in two phases. In the first phase, a lens body is heated to the lithium melting temperature and then low pressure argon gas is applied to aid in lithium removal. In the second phase, water is circulated through the room temperature lens body to react with and remove remaining lithium from surfaces of the steel and titanium structures. A third phase involves the recombination of hydrogen released from the second phase by controlled combustion. The collection and analysis of the resulting water vapor may shed some light on the production of gases such as helium, and hydrogen resulting from the interaction of the particle shower with lithium.

A conceptual design for lens unfilling process was developed in the fourth quarter of 2000. The process was reviewed by the BD ES&H Department and the ES&H Section and preliminary approval of the process was given in the first quarter of 2001. Testing for two of the three phases of the process was completed in the first quarter 2001. The work is required to be conducted within a controlled atmosphere and consequently, a glove box was procured for this purpose in the second quarter of 2001. Final process development, equipment setup, and safety approval are expected to be completed in the second quarter of 2001. The first lens unfilling should be completed during the second quarter of 2001. Unfilling of the remaining four lens should be completed early in the third quarter of 2001.

- FEA of Current Lens Design

FEA of the current lens design is almost complete. Stress and deflection results have been generated for several load cases. The results are currently being reviewed and will most likely be written up in a P-Bar Note. Preliminary results show that the current lens pulsed at 670 kA (10 Tesla surface field) may have problems with septum/lithium separation. In addition, two areas of the septum exhibit large stress reversals that encroach upon endurance limits of the material (Ti 6Al-4V ELI). There is also some indication that the center body to septum seal area undergoes large deformation and/or stresses which could result in lithium leakage at the seal.

- New High Gradient Solid Lens Design

- Lens/Beam Physics Modeling

Significant progress has been made in producing the collection lens model. Most of the programming work required for the MARS modeling work has been completed. Magnetic field calculations have been made using the program ANSYS and the results of those calculations have been incorporated in the MARS model so that end effects are now considered. Some, but not all, of the experimental data compare well with preliminary MARS calculations. At this time, there is a small amount of work remaining to define the acceptance of the AP2 line and Debuncher. In addition, more programming work is planned to improve the ease of use by the end user. The MARS modeling effort should be well understood and completed by the end of June 2001. Documentation of the MARS model and further improvements will continue through the third quarter of 2001. Quantitative comparisons of production efficiency of the existing and future designs will be possible by the end of May 2001.

- FEA of New Lens Designs

An FEA model of a prototype high gradient lens has been created and is in the initial stages of analysis (see description of first prototype design below). It is expected to be only a matter of a few weeks before results from this analysis are available.

- Diffusion Bonded Septum Joints

Diffusion bonding technology has been used to manufacture several sample joints for metallurgical analysis. From this work a joint design has been chosen as being optimal for the most critically stressed joint in the septum (inner conductor tube joint). This joint design exhibits good grain growth across the bond line, good microstructure for strength, and minimal stress concentration features (crack initiation sites) at the surface. Manufacture of the samples also resulted in the realization that, if the lens body is also made out of titanium alloy, both the body

and the septum can be joined as one diffusion-bonded component. This should result in a much faster and cost effective joining process, not to mention that it eliminates a critical lithium seal. Currently 30 joint samples are being prepared for fatigue testing to determine the joint's endurance limit for fatigue.

- Prototype Program

Time constraints have required the design of a prototype high gradient lens before all the design data have been determined (it will take several months for fatigue testing joints for instance). However, using the preliminary data currently available a reasonable first prototype can be designed and constructed that will yield valuable experience with the diffusion bonding process and indicate if identified design improvements are beneficial. This prototype is in the final stages of design. It uses a 0.8 cm radius central lithium conductor (previously 1 cm) with a 1.5 mm titanium alloy septum wall (1 mm previously). It will be constructed via diffusion bonding which results in a water-cooled titanium alloy body. The body and septum are one-piece which eliminates the troublesome lithium seal between body and septum. It is also interesting to note that the diffusion-bonded design precludes the inclusion of lithium 'buffer' volumes that were part of the previous design. Manufacture of parts should begin within the next two weeks.

- Lens Filling Research and Development

The entire lens filling instrumentation system has been re-engineered to achieve better signal to noise ratio and increase sensitivity. Several tests have been run with the instrumentation system to ensure its robustness during a fill. A 'dummy' lens is currently being assembled that uses an actual old lens assembly to mimic the fill process with hydraulic oil. Thus the fill process can be simulated many times and calibration of instrumentation at various pressures and temperatures can be performed. Compression testing of lithium has also been conducted to aid in the understanding of lithium behavior during the fill process. This information also came in useful for the lens FEA described earlier. It is planned to start using the dummy lens in calibration runs over the next few weeks. Work on pre-load adjustment schemes has not progressed beyond the conceptual design stage.

### 3.3.1.2 *Liquid Lithium Lens*

#### 3.3.1.2.1 Scope

Collaboration between Fermilab and the Budker Institute of Nuclear Physics in the form of an Accord was begun in July 1997. The purpose of the Accord is to explore the feasibility of producing and operating a collection lens containing a liquid lithium conductor. It has been postulated that the current solid lithium collection lens operation is limited in part due to complications arising from the rate of heat removal from the lithium conductor. Significant heating of the lithium conductor occurs during the electrical current pulse. In the solid lens design, heat removal is accomplished by water-cooling jacket contained within the solid lens assembly. In the liquid lithium lens design, heat deposited by the current pulse is removed by continuous pumping of the liquid lithium from the lens body to an external heat exchanger. It is also believed that in the solid lens, the lithium conductor becomes separated from the inner

titanium conduction tube due to a magnetic pinch which occurs at or below design gradient. The separation of lithium from the inner conductor wall could lead to arcing in the lithium conductor, poor heat transfer, and high level cyclic stresses. In the liquid lithium lens, it is believed that the pressure of the lithium piping system can be controlled to prevent the separation of lithium from the inner conducting tube. The liquid lithium project as currently conceived, requires of a number of auxiliary external support systems to pump liquid lithium, control system pressure, lithium flow and lithium temperature. These systems represent significant complications to target station operation.

#### 3.3.1.2.2 Status

The work outlined in the Accord is divided into four phases. Phase 1 included the performance of engineering calculations and conceptual design work. Additional design work and construction of components including a lens power supply were to be completed in Phase 2. In Phase 3, the goal is to operate a lens for 1 million pulses at a surface field of 13 Tesla. The purpose of testing a lens at such high gradient is to ensure that operation at a surface field of 10 Tesla would be reliable for many millions of pulses. In addition, the tested lens, power supply, lithium pumping and pressure control systems and lens control systems are to be delivered to Fermilab. Finally in Phase 4, a second untested lens of the same design is to be built and shipped to Fermilab.

Phases 1 and 2 are considered to be more or less complete. Phase 3 is currently ongoing. To date, two lens designs have been attempted and have failed. In a review held at Fermilab during the week beginning April 9, 2001, we learned that testing of a 3<sup>rd</sup> generation lens will begin at BINP in May/June 2001. It is planned to ship a lithium pumping system equipped with locking valves, pressure control system, and system controls to Fermilab in July/August 2001. At the same time, a power supply designed for operation of either a solid lens or a liquid lithium lens will be shipped to Fermilab. The delivery of the tested lens will depend on completion of successful testing. The purpose of shipping the lithium contour and associated controls, perhaps in advance of delivery of a successful lens, is to get Fermilab involved in the operation of a liquid lithium system so that experience with system operation can begin to accrue.

The original Accord, which was signed in July 1997, was scheduled at that time to be completed during the year 2000. Unforeseen difficulties in this work have delayed its timely completion. At this time, an amendment is being prepared to provide additional funds to BINP to allow continued work for tasks outlined in Phase 3. Given sufficient time and resources, there is no reason to believe a liquid lithium lens can not be produced. At this time however, it is not clear that sufficient time is available to complete the liquid lens project in time for RUN IIB. If testing of a liquid lithium lens is eventually successful, significant resources will be required to configure a liquid lithium lens system into the modular form required for target vault operation.

#### 3.3.1.3 *Beam Sweeping*

##### 3.3.1.3.1 Scope

Antiprotons are produced from the interaction of a 120 GeV proton beam from the Main Injector with a nickel target. Quadrupole magnets focus the incident beam on the target, a smaller beam

spot increases the antiproton collection efficiency. The production target used through much of Collider Run I was made of copper. When intensities in the old Main Ring reached their peak at around  $3.25 \times 10^{12}$  protons per pulse (ppp), measurements indicated that melting occurred during the beam pulse and adversely affected the yield. Though the reduction in yield was only a few percent, it became clear that a change in target material, spot size or beam position would be required for running at intensities expected in the Main Injector era without a significant reduction in yield. The penalty for increasing the energy deposition beyond the melting point would not only be reduced yield, but possible damage due to the shock waves developed in the target during the beam pulse.

During the latter part of Collider Run I, nickel targets began to be used in place of the copper targets. Nickel is similar in atomic structure to copper, so the optimum target length and yield characteristics of the two materials are nearly identical. Nickel has the advantage that the onset of melting requires nearly twice the energy deposition as copper. In addition, nickel is more tolerant of the shock waves that will develop during the beam pulse. Without a beam sweeping mechanism in place, the spot size on the target would be increased to prevent damage. The increased spot size would reduce antiproton yield 5-10% at  $5 \times 10^{12}$  ppp (Main Injector design intensity) and 15-20% at  $9 \times 10^{12}$  ppp (slip stacking).

The idea of sweeping the proton beam across the target to reduce peak heating is not a new one, the Tevatron I design report included beam sweeping as a future upgrade. The design phase of the sweeping project began in 1995 and included several years of research and development. Early sweeping designs made use of kicker style magnets similar to those used in the accelerators. In the final design, the sweeping magnets have conductors rotated about the beam axis to generate a rotating dipole field. The power supply required to provide the bipolar magnet current pulse involves two-stage compression with saturated reactors.

The targeted beam needs to be moved about 0.3 mm during the  $1.6 \mu\text{s}$  beam pulse to adequately distribute the beam energy. Sweeping magnets are required both upstream and downstream of the target to preserve the proper trajectory of the antiprotons entering the AP-2 line. There are a pair of upstream sweep magnets and a single downstream sweep magnet because the proton beam has an energy of 120 GeV and the antiproton beam is only 8 GeV. There are differences in the striplines and other external details of the downstream magnet in the vault as compared to the upstream magnets located in the AP-1 line.

#### 3.3.1.3.2 Status

When the beam sweeping project was begun, it was scheduled to be completed in parallel with the construction of the Main Injector. The project is behind schedule at this point, although most of the major fabrication has been done. The sweeping magnet power supplies are essentially a custom design and many of the components were not available commercially. All of the personnel originally involved in the project have left Fermilab so there have been inefficiencies due to lack of experience.

Presently, one of the bipolar power supplies has been test pulsed approximately 2 million times. This power supply is being tested with the downstream module, stripline and magnet assembly at APO. The other two power supplies for the upstream magnet are nearing completion and will begin their testing phase during the early summer 2001. If there aren't any major component failures during the testing phase, the power supplies will be deemed operational. There is also a rather complex stand-alone controls system that keeps the upstream and downstream magnet synchronized. It will be tested at APO with the existing test setup.

The magnets and stripline assemblies have had several design flaws that have required attention. In some cases, a total redesign has been required to make the components functional. A request was made to keep the upstream sweeping magnets under vacuum, requiring the design and fabrication of a ceramic beam pipe. Finally, the magnet and stripline assemblies appear to be nearing completion. A realistic goal would be to have them ready for installation in the tunnel during summer 2001.

Despite the delays in implementing the sweeping system, it hasn't caused a serious reduction in antiproton yield yet. As the Main Injector intensity increases from the  $4E12$  ppp peak intensities experienced through spring 2001, the reduction will be more noticeable. After the power supplies, magnet assemblies and other components are completed, testing with beam will commence. Prior to installing the downstream sweeping magnet in the vault, the upstream sweeping magnets will be installed and tested with beam. The secondary emission monitor located just upstream of the target and beam position monitors in AP-2 can be used to detect beam motion. After confidence is gained in the upstream magnets, the downstream magnet can be installed and the testing phase completed. The downstream magnet will be located in an extremely radioactive environment. Once it is in place, it will be difficult to do any significant mechanical modifications due to residual radiation. The goal would be to enter the beam testing phase in the late summer or fall 2001, with the system operational the following winter.

### **3.3.2 Debuncher**

#### *3.3.2.1 Aperture*

The Debuncher magnetic elements were designed to have 40pi mm-mrad apertures. The beam pipe and other Debuncher elements are the aperture limitations and measurements of ~25pi mm-mrad have been observed in each plane. Studies to identify aperture limitations will be on going and improvements will be implemented as opportunities are presented. To perform the aperture studies, the diagnostics and orbit control will need to be improved.

Most of the needed Debuncher diagnostics for aperture studies are working. The beam loss monitors and scrapers are functional. The beam position monitor system (120 BPMs) needs to be upgraded. The original BPM electronics, including the Z80 based data acquisition system, are still used. An upgrade of the BPM electronics and data acquisition will provide better precision and improved reliability. Instead of a multi-purpose BPM system capable of both closed orbits and turn-by-turn, a new system will focus on closed orbits. Since the BPM system is used during

studies periods and the Debuncher is non-ramping, a simple BPM system can be implemented. A simple tuned receiver is being considered along with using a commercially available data acquisition system.

The installation of the Debuncher Run II cooling upgrade tanks required the removal of many trim dipole magnets; 11 horizontal and 6 vertical trims remain in the well-packed Debuncher ring. Recently, 5 two-plane motion controlled quadrupole stands were installed. Local bumps have been successfully implemented by using a combination of movable quads and trims. Ten more movable quad stands are being built and will be installed this summer. Another 20+ additional movable quad stands would be needed to have a complete set of local bumps about the Debuncher ring.

As aperture limitations are identified, fixes will be implemented. If indicated, the beam pipe within accelerator components will be replaced and the new vacuum chamber will be made as large as possible. It may be necessary to replace the dipole magnets' vacuum chambers: curved pipe would replace welded straight segments which currently inhabit the dipoles. In some cases, components may have to be redesigned to increase the aperture.

### 3.3.2.2 Lattice Upgrades

The aperture improvements of section 3.3.2.1 presuppose a Debuncher that is capable of performing all of its functions on beam that is spread out over a significantly greater phase space area than what has been achieved in the operational history of the Antiproton Source. The lattice upgrades described in this section are intended to enhance the performance of the Debuncher within the present aperture and ensure that maximum use is made of the Run IIb aperture improvements.

Therefore, there are three basic motivations for the proposed Debuncher Lattice upgrades:

- 1) Ensure that the dynamic aperture of the Debuncher exceeds the physical aperture that is achieved by way of the aperture upgrades of the previous section
- 2) Optimize the lattice for stochastic cooling
- 3) Optimize the lattice for RF bunch rotation

Four different lattice improvements are currently under consideration. They are:

- Betatron coupling correction
- Resonance correction
- $\gamma_{\tau}$  ramp

A number of beam studies are planned to determine the impact of these improvements on the performance of the Debuncher during antiproton stacking. These studies are described in each of the sections below

#### 3.3.2.2.1 Betatron Coupling Correction

##### ➤ Scope

The Debuncher lattice contains no provision for the correction of skew-quadrupole errors. Skew-quadrupole errors cause coupling of the horizontal and vertical betatron motion of the beam and consequent increased transverse beam size.

It has been established that some amount of skew-quadrupole error is present in the Debuncher lattice. Coupling of the horizontal and vertical motion can be seen in observations of the Debuncher betatron sidebands (see **Figure 3-6**).

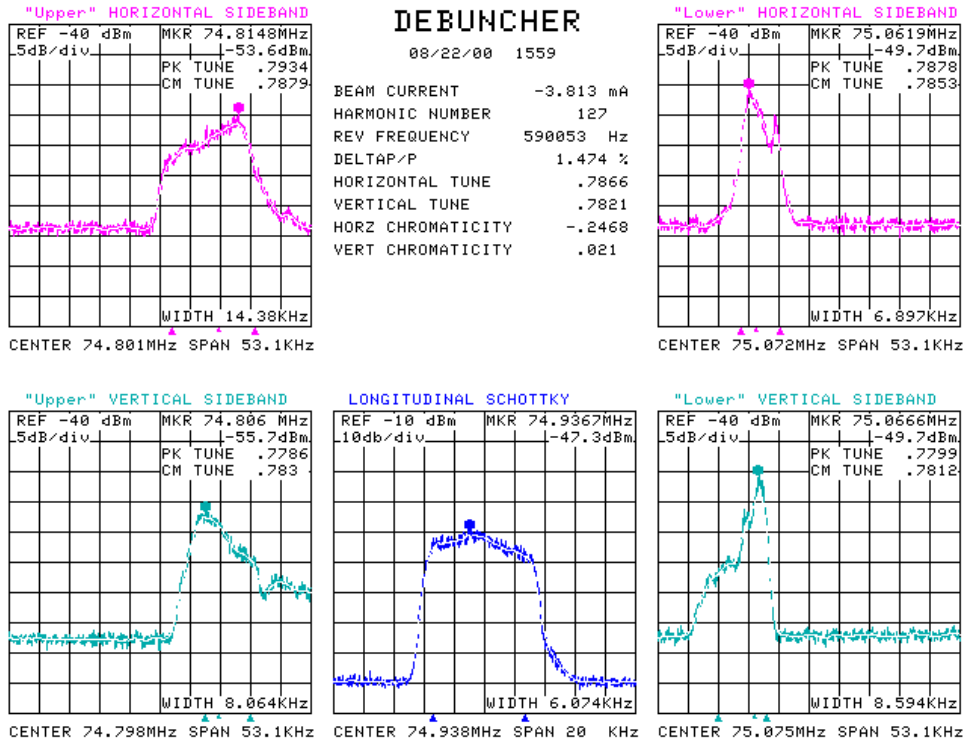


**Figure 3-6** Debuncher tune measurements. The upper right and left spectra are from the Debuncher horizontal schottky detector. The lower right and left spectra are from the vertical schottky detector. The presence of coupling is particularly apparent on the lower sideband measurements where the narrower distribution in one plane gives rise to a distinct structure in the spectra of the opposite plane.

The correction of coupling requires the addition of two skew-quadrupole magnets to the Debuncher lattice. Ideally, these magnets should be located 90° in “coupling phase”† from one another. If coupling correction is necessary, the construction, testing, installation and commissioning of the skew-quad correctors will be included in the scope of the Debuncher lattice upgrade project.

#### ➤ Studies

The first studies to be done are tracking studies with a model of the Debuncher lattice. Such a study will determine if coupling correction is required. If coupling correction is deemed necessary, further studies with beam will be required to measure the amount of the coupling error present so that the strength of the correction skew-quadrupoles can be determined.

† Coupling phase,  $\phi_c$ , is given by:  $\phi_c = \phi_x - \phi_y$ , where  $\phi_x$  and  $\phi_y$  are the horizontal and vertical betatron phase advance at any given point in the lattice.

### 3.3.2.2.2 Resonance Correction

#### ➤ Scope

The Debuncher drives the fourth order non-linear resonances (see **Figure 3-7**). The operating point of the Debuncher is sufficiently close to  $9\frac{3}{4}$  in both planes that these resonances are at least an occasional operational annoyance. The strategy for dealing with the fourth order resonances to date has been to maintain the Debuncher tunes as far away from  $\frac{3}{4}$  as possible. The tunes in both planes must be sufficiently far from the resonance lines for beam at any place in the momentum aperture to avoid beam loss. There is also evidence that beam is lost at the edge of the momentum aperture (see **Figure 3-8**), although it is not known that this loss is due to any of the fourth order resonances.

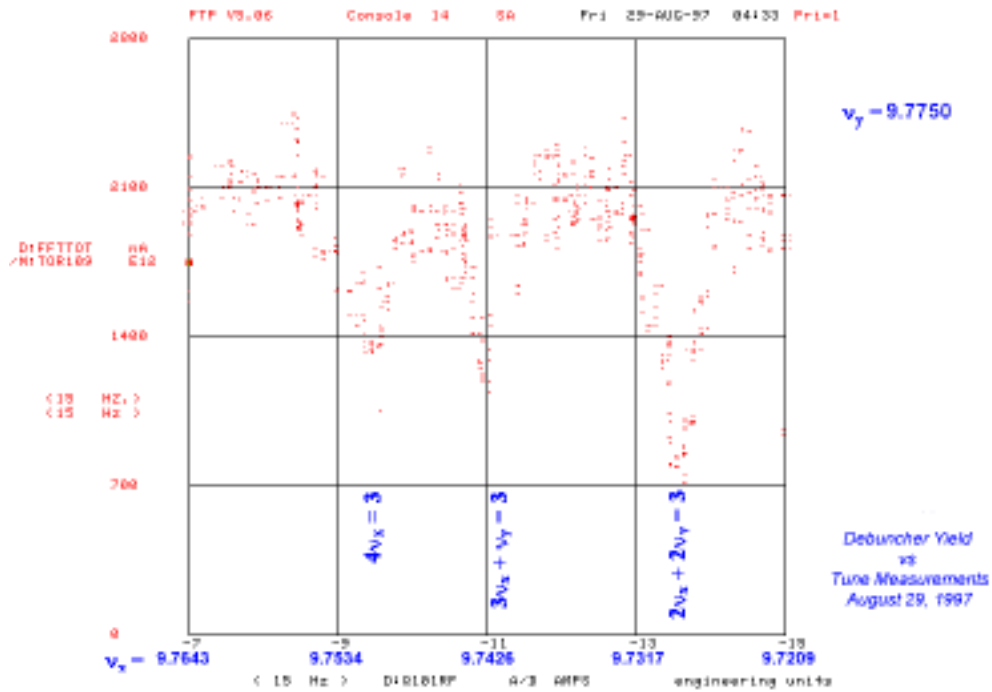


**Figure 3-7** Measurement of  $\bar{p}$  yield into the Debuncher during stacking versus horizontal tune. The vertical tune was held constant at  $v_y = 8.775$ . The dips in the yield occur at three of the 4<sup>th</sup> order horizontal resonances.

The first step of this component of the Debuncher lattice upgrades is to ascertain the impact of the fourth order resonances on the performance of the Debuncher. The second step is the implementation of octupole circuits to correct the resonances that interfere with efficient operation of the Debuncher. If 4<sup>th</sup> order resonance correction is necessary, the construction, testing, installation and commissioning of the octupole correctors will be included in the scope of the Debuncher lattice upgrade project.

➤ Studies

A couple of beam studies can be performed to determine the severity of the fourth order resonances in the Debuncher.

- 1) During stacking, measure the  $\bar{p}$  yield into the Debuncher versus tune for all five 4<sup>th</sup> order resonance lines along two paths in tune space: (i) vertical tune fixed, vary the horizontal tune (except the  $4\nu_y = N$  resonance); (ii) horizontal tune fixed, vary the vertical tune (except the  $4\nu_x = N$  resonance).

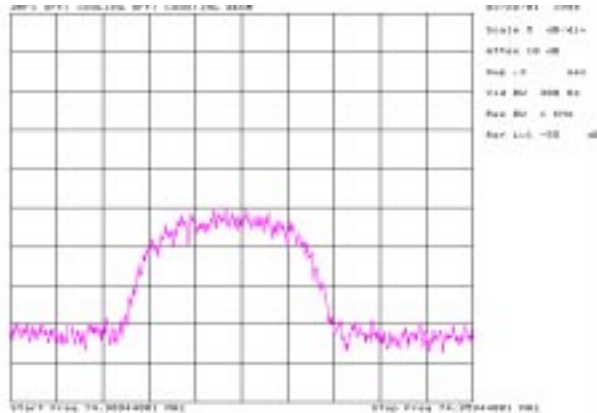


**Figure 3-8** Longitudinal distribution of newly injected  $\bar{p}$  beam in the Debuncher during stacking. Bunch Rotation RF has been turned off and de-tuned. Stochastic cooling is off. Under these conditions, the beam should fill the momentum aperture of the Debuncher. The less than sharp edges of this distribution indicate that beam has been lost at the edges of the momentum aperture. Some of this loss may be due to 4<sup>th</sup> order resonances.

Date: 07-16-99 Time: 06:57 AM

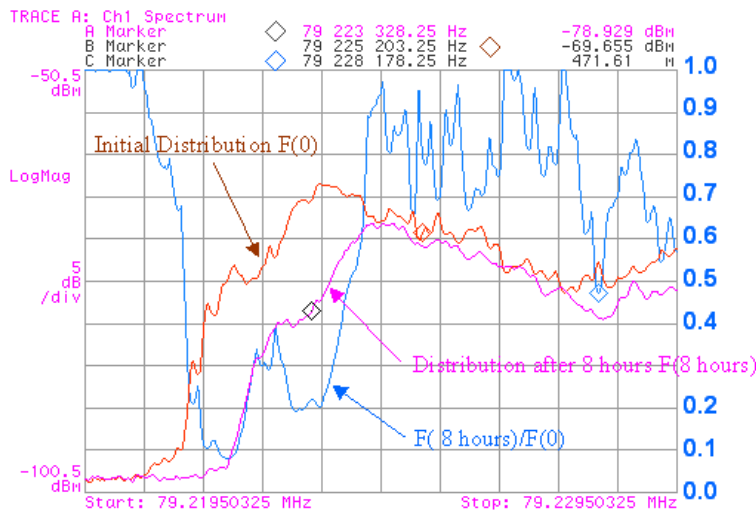


**Figure 3-9** Measurement of beam lifetime versus  $\Delta p/p$  near the high-energy end of the Accumulator momentum aperture. The horizontal axis is  $126 \times (\text{Revolution Frequency})$ , which is related to  $\Delta p/p$ . In this measurement, beam with a large momentum spread near the high-energy side of the Accumulator was left circulating for 8 hours. The orange trace is the initial distribution; the purple trace is the distribution after 8 hours; the blue trace is the ratio of the 8-hour distribution to the initial distribution.

2) Measure the tunes in each plane as a function of  $\Delta p/p$  relative to the central orbit. Measure the beam lifetime in the Debuncher as a function of  $\Delta p/p^\ddagger$ . Determine what resonance lines correspond to any dips in a graph of lifetime versus  $\Delta p/p$ .

This measurement can be performed with beam that is initially spread out to fill the momentum aperture of the Debuncher. The relative loss after a given amount of time versus  $\Delta p/p$  is then measured. **Figure 3-9** shows a similar measurement of this kind made with beam near one edge of the Accumulator momentum aperture.

This measurement should be repeated for a variety of central orbit betatron tune combinations.

### 3.3.2.2.3 $\gamma_t$ ramp

#### ➤ Scope

The purpose of the Debuncher is two-fold. First, the Debuncher must remove the 53 MHz RF modulation of the beam, and second, the Debuncher must compress the beam in phase space so that it can be efficiently transferred into the Accumulator and captured with the stacking RF system. The first task is accomplished by an RF bunch rotation where the initial narrow time structure and wide energy spread is rotated  $90^\circ$  in longitudinal phase space into DC beam with a relatively narrow momentum spread. The Debuncher's second function is accomplished by transverse and longitudinal stochastic cooling. RF bunch rotation and stochastic impose conflicting constraints on the Debuncher lattice. In particular, different constraints are imposed by each process, on the machine parameter  $\eta$ .  $\eta$  is related to the transition energy by

$$\eta = \frac{1}{\gamma_t^2} - \frac{1}{\gamma^2}$$

$\gamma_t m_p c^2$  is the transition energy of the accelerator.

Bunch rotation requires an RF bucket sufficiently large to capture the entire momentum spread of the beam, which in turn requires a small value of  $\eta$ . Stochastic cooling requires that the beam dipole moment and momentum spread sampled by the pickups on each turn be statistically independent, which in turn requires a relatively large value for  $\eta$  for efficient mixing. The design value of  $\eta = 0.006$  is a compromise between these two requirements.

It may be possible to improve on the present situation by changing the value of  $\eta$  during the stacking cycle by ramping  $\gamma_t$ . An initial attempt to improve cooling by increasing  $\eta$  during the stacking cycle was made in 1995\*. The  $\gamma_t$  ramp has not been implemented as a normal part of Debuncher operation due to the difficulties that were encountered in rapidly ramping the Debuncher quadrupole magnet power supplies. The regulation errors during ramping caused unacceptably large tune excursions. It is clear, therefore, that the implementation of a  $\gamma_t$  ramp in the Debuncher will require a significant amount of power supply re-engineering.

A significant benefit of lowering  $\eta$  early in the stacking cycle is an increase in the momentum aperture of the Debuncher at the very time when the momentum spread of the beam fills the

---

<sup>‡</sup> In this section,  $\Delta p/p$ , unless otherwise indicated, refers to a deviation in momentum relative to the central orbit.

\* D.A. Olivieri, *A Dynamic Momentum Compaction Factor Lattice for Improvements to Stochastic Cooling in Storage Rings*. Ph.D. Thesis. University of Massachusetts, Amherst (1996).

aperture. The relationship between the momentum deviation of a beam particle,  $\Delta p$ , and its average radial displacement from the central orbit,  $\Delta R$ , is given by:

$$\frac{\Delta p}{p} = \gamma_t^2 \frac{\Delta R}{R}$$

If  $\gamma_t$  is changed and the limiting aperture in the Debuncher remains the same\* then the maximum accepted  $\Delta p$  changes according to:

$$\frac{\Delta p_{new}}{\Delta p_{old}} = \left( \frac{\gamma_t^{new}}{\gamma_t^{old}} \right)^2$$

Thus if  $\gamma_t$  is increased, the momentum aperture increases. If  $\gamma_t$  is increased such that  $\eta$  changes from its design value of 0.006 to 0.003, the momentum aperture increases by a factor of 1.2.

### ➤ Studies

A significant part of this section of the Debuncher lattice upgrade is to determine, both theoretically and by beam measurements, the expected increase in the antiproton stacking rate that would result from the implementation of a  $\gamma_t$  ramp. At the present time, the impact on stacking from a change in the value of  $\eta$  in the Debuncher is not well understood.

**Figure 3.10** shows the model prediction of bunch rotation performance as the bunch length of the rotated beam is varied. The model indicates that the reduction of  $\eta$  by a factor of 2 would not improve bunch rotation unless the bunch length (or longitudinal emittance) in the Main Injector is substantially below 1 nsec and second harmonic correction is added to the Debuncher RF system. It is imperative that the model be checked with beam measurements before proceeding further with any plans to lower  $\eta$ .

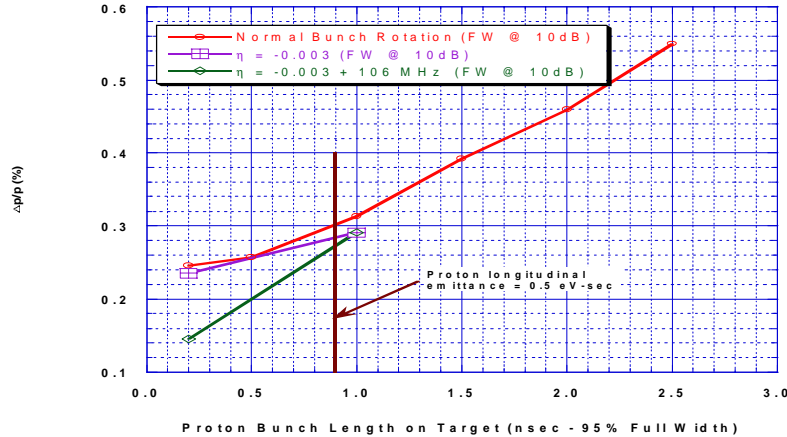


**Figure 3-10** Results of an ESME model of bunch rotation in the Debuncher. This plot shows the  $\Delta p/p$  after bunch rotation versus the bunch length of the protons on target. The red graph is the model for the present Debuncher lattice ( $\eta = 0.006$ ). The purple graph shows the expected bunch rotation performance if  $\eta$  is decreased to 0.003. The green trace shows the bunch rotation performance if 2<sup>nd</sup> harmonic correction (106 MHz) is added to the bunch rotation RF system. The vertical brown line shows the minimum expected bunch length when slip-stacking is implemented.

\*In addition, it is assumed that the beta functions at the location of the limiting momentum aperture don't change appreciably.

A second category of beam studies is the measurement of the impact of a lower post-rotation  $\Delta p/p$  on the cooling rates in all three dimensions. Since the kicker to pickup mixing is inversely proportional to the momentum spread of the beam, some or all of the benefit of improved bunch rotation performance may be lost due to subsequent reduced cooling rates from poorer mixing.

### 3.3.3 Accumulator

#### 3.3.3.1 Accumulator Cooling for Run IIb

With the increased antiproton flux into the Accumulator, we will need to upgrade both the longitudinal and transverse stochastic cooling systems. The current 2-4 GHz stacktail cooling system, which moves the injected beam from the deposition orbit to the core, was designed to have a maximum flux of 30-35 mA/hour. Changes in the pickup design, as described below, and reduction in the operating temperature (from current liquid N<sub>2</sub> temperature to liquid He temperature) will be necessary to handle a flux of 60 mA/hour or greater. We have core transverse cooling systems in both the 2-4 GHz and 4-8 GHz bandwidths. The sensitivity of these systems may need to be increased. Currently, there are no stacktail transverse cooling systems, only core transverse cooling systems.

#### 3.3.3.2 Description of stochastic stacking

Stochastic stacking with a constant flux is achieved by designing a system with gain as a function of energy that falls exponentially, with characteristic energy  $E_d$ . The resulting maximum flux  $\Phi$  can be expressed as:

$$\Phi = \frac{W^2 \eta E_d}{f_0 p \ln\left(\frac{F_{\min}}{F_{\max}}\right)},$$

where  $W$  is the bandwidth of the system,  $\eta$  is the phase slip factor,  $f_0$  is the beam revolution frequency,  $p$  is the beam momentum, and  $F_{\min}$  and  $F_{\max}$  are the minimum and maximum frequencies in the system bandwidth. Planar pickups have a response which goes like  $\exp(-\pi x/d)$ , where  $x$  is the transverse distance from the center of the pickup and  $d$  is the vertical aperture. If the pickups are located in a region of high momentum dispersion, we can design a system where the gain response falls off exponentially with energy. In **Figure 3-11**, we show the antiproton density distribution, as a function of beam revolution frequency, overlaid with an exponential fit. We use the fit result to calculate the flux for this particular stack size. In **Figure 3-12**, we show the fitted flux result versus stack size for two different stacking periods. Note that the fitted maximum flux, based on the slope, is on order 30 mA/hour even though the stack rate was about 10% of that number.

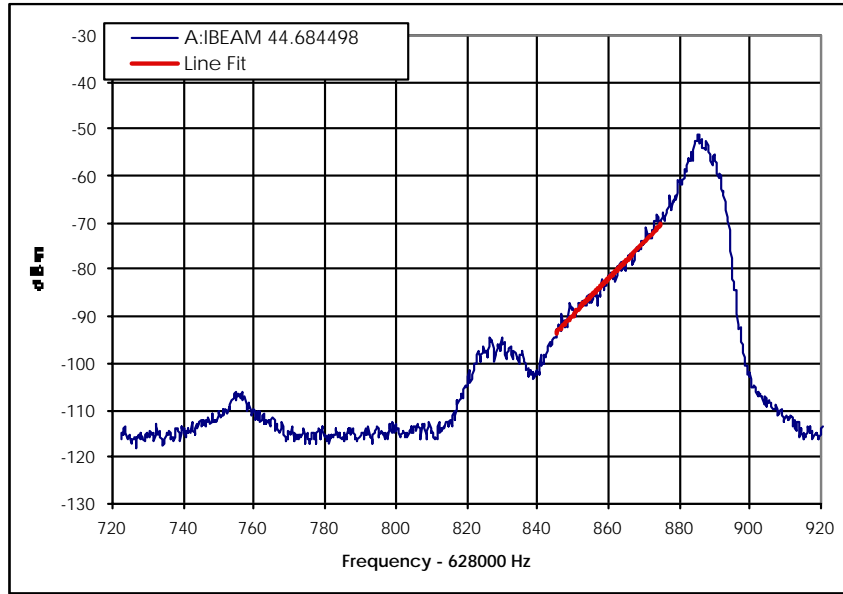


**Figure 3-11** Stacking density distribution overlaid with exponential fit.

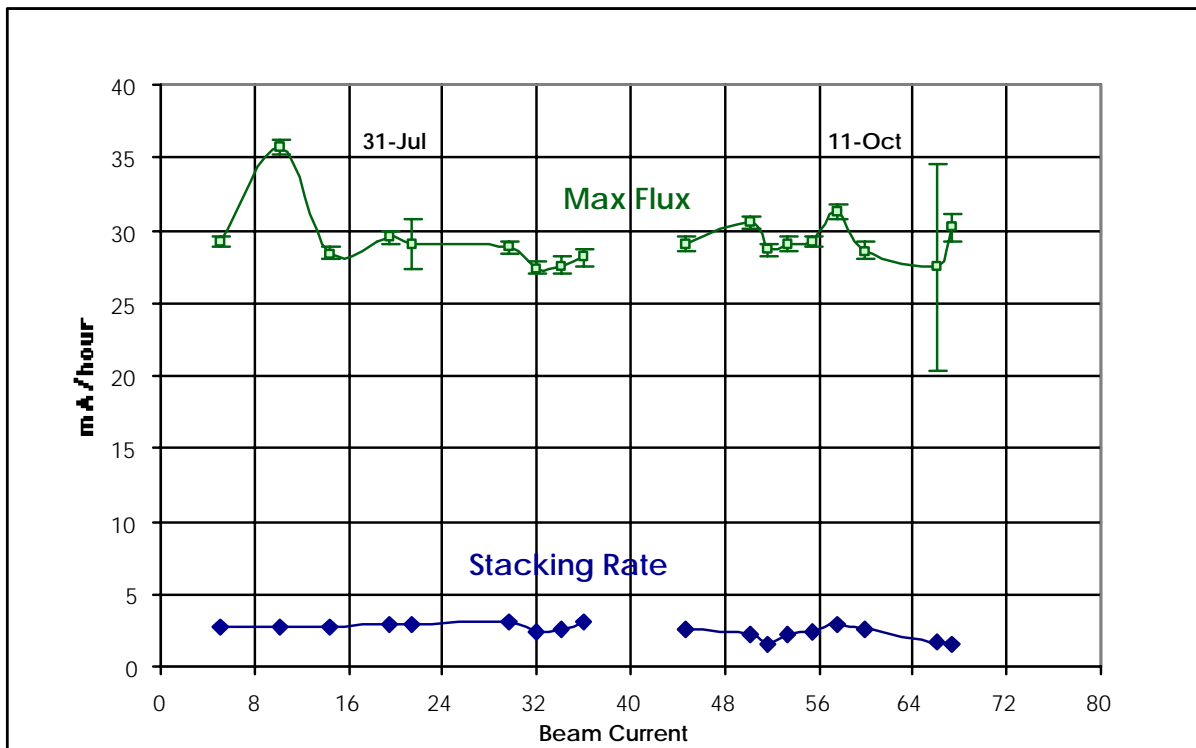


**Figure 3-12** Flux results (mA/hour) vs stack size

By changing the vertical aperture at the pickup location, we can change the characteristic energy  $E_d$  and hence the maximum flux through the system.

Detailed simulations of the current stacktail system have been performed. The peak performance agrees well with the predicted 30 mA/hour maximum flux. In **Figure 3-13**, we show the simulated performance. An input flux of 50 mA/hour was used. After a short time period, the system reached a stable stacking rate of 28 mA/hour.

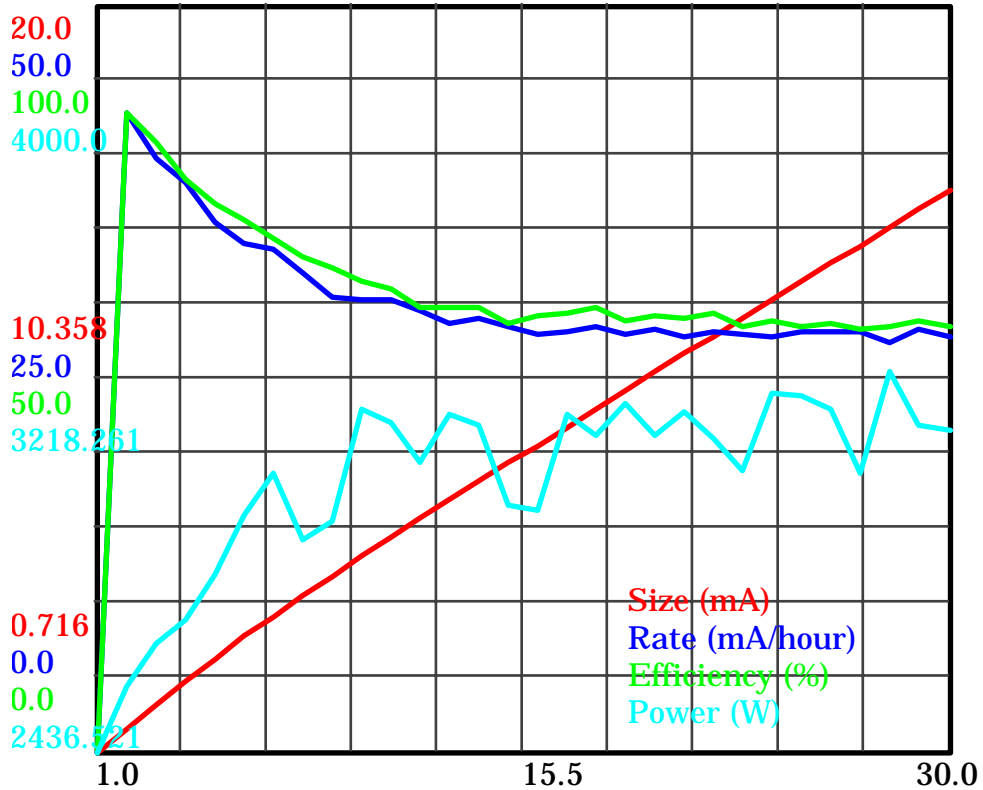


**Figure 3-13** Simulated performance of Run II stacktail cooling system. Horizontal scale is time in minutes.

As a possible upgrade, we changed the simulation vertical aperture at the pickup position by a factor of 1.67, going from the nominal 3.3 cm to 5.5 cm. This change should give a direct factor of 1.67 in maximum flux, all other things being equal. We find that the maximum flux achievable in this design is on order 45 mA/hour, an increase of a factor of 1.6 over the current design. We believe that the upgrade does not reach the desired factor of 1.67 because of problems with system noise.

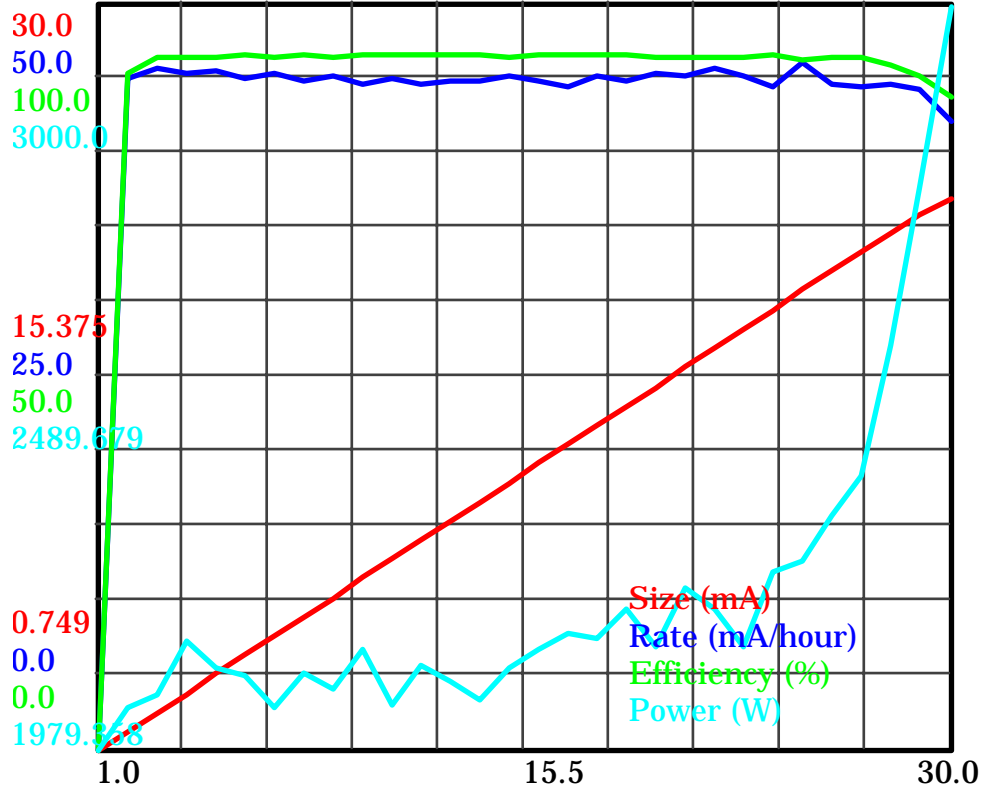


**Figure 3-14** Simulated performance of upgraded stacktail cooling system. Horizontal scale is time in minutes.

By increasing the vertical aperture by a factor of 1.67, we have lowered the pickup sensitivity by a factor of 0.84. We therefore need to increase the gain to move the beam off the deposition orbit (before the next pulse shows up). We have changed the value of  $E_d$  by a factor of 1.6, so the stacktail gain profile falls more slowly and the core cooling gain needs to be increased to match the value of the stacktail. This is a significant change, on order 10 dB, and changes the performance of the core cooling significantly. The large rise in power after 20 minutes that is visible in **Figure 3-14** is a result of the core cooling being overwhelmed by the beam density and the noise. Though it has not been simulated, we believe that to increase the maximum flux an additional 33% (reaching to 60 mA/hour) we will have to reduce the operating temperature of the stacktail and core cooling systems to ~10 K (as achieved in the Debuncher Run II cooling) with liquid He.

The large rise in power also points to the requirement of frequent transfers of the antiprotons from the Accumulator to the Recycler. For efficient transfers, we need a small momentum spread in the antiprotons. In **Figure 3-15** and **Figure 3-16**, we show the density distributions after 10 and 30 minutes respectively. After 10 minutes, there is a well-developed, small momentum spread core which could be transferred to the Recycler. After 30 minutes, the core has gotten significantly wider and it would be much more difficult to transfer.

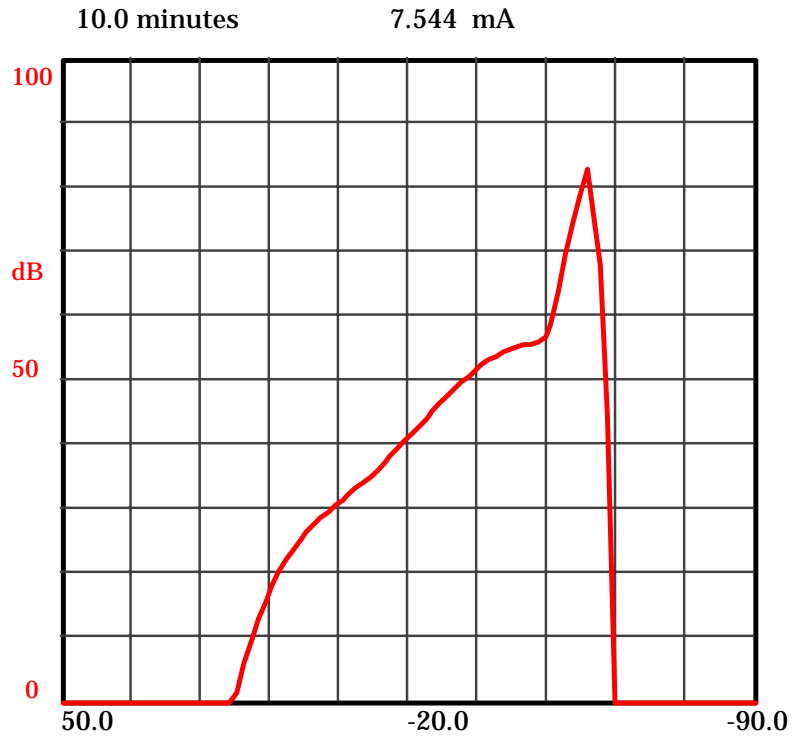


**Figure 3-15** *Density after 10 minutes.*

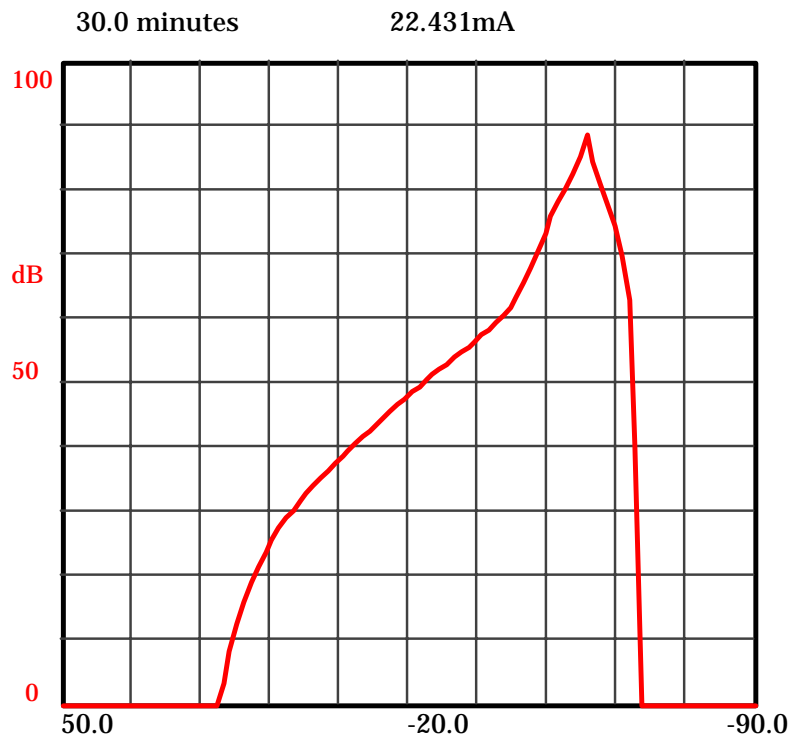


**Figure 3-16** *Density after 30 minutes.*

To get the desired 60 mA/hour flux, we plan on increasing the aperture of the stacktail cooling pickups from 3.3 cm to 6.6 cm. As described above, we will accompany this change with a change in the operating temperature, with a goal of 10 K or smaller. We have not begun any of the engineering design for these new pickups, though our experience with the Debuncher Run II pickups gives us confidence that it can be built and operated. In the coming year, we plan on performing additional simulations to investigate the performance with the doubled aperture

## 3.4 Recycler

### 3.4.1 Electron Cooling

#### 3.4.1.1 Background

The Laboratory started in 1995 to investigate the application of electron cooling to 8.9 GeV/c antiprotons in the Recycler as a promising component of an upgrade of Tevatron luminosity beyond the Run IIa goals. The idea was not entirely new at that time; it had been proposed as an upgrade path for the Accumulator as early as 1985 [5], and there had been some experimental work as well as conceptual development [6]. The practice and principles are well established for ions with velocity less than  $0.8 \cdot c$ , i.e., for p-bars of less than a GeV or so. For ions of higher velocity the fundamentals are the same, but hardware development is required and the technical problems differ.

The Recycler is a fixed 8 GeV kinetic energy antiproton storage ring, installed near the ceiling of the Main Injector tunnel. It employs a stochastic cooling system to collect multiple batches from the Accumulator and re-cool antiprotons, which remain at the end of Tevatron stores. Electron cooling will improve cooling performance in the Recycler, permitting faster stacking and larger stacks. In combination with other accelerator upgrades it will permit substantially greater luminosity in the collider. The Recycler electron cooler, discussed here, will be installed in the MI-30 section of the Recycler tunnel and it is schematically shown in **Figure 3-17**.

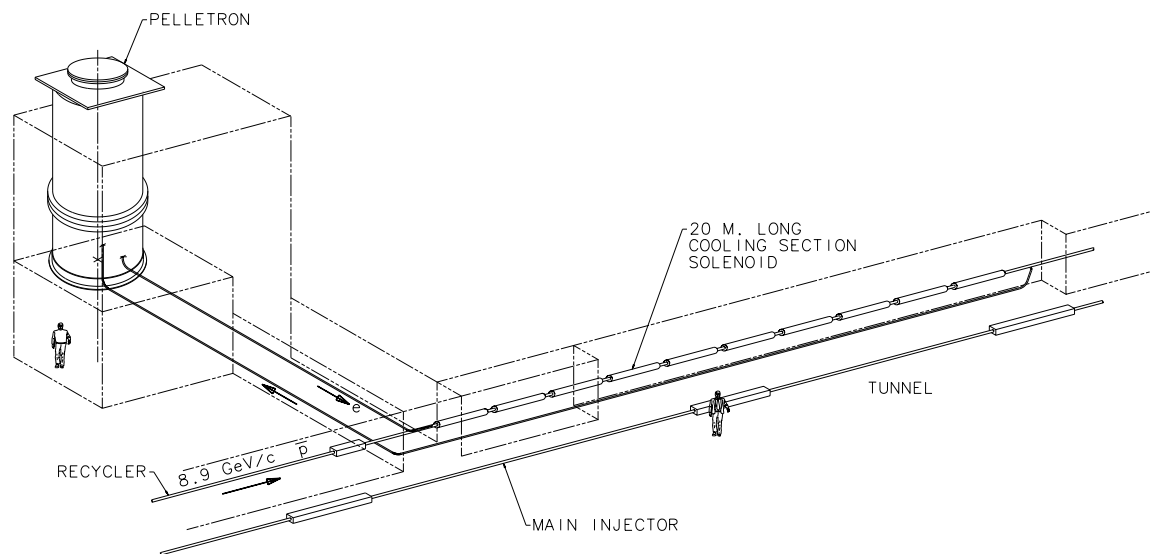


Figure 3-17 Schematic layout of the Recycler electron cooling system.

A charged particle (i.e. an antiproton) traveling in an electron beam undergoes Coulomb scattering with the electrons. The resulting friction and velocity diffusion tend to bring such

particles into thermal equilibrium with the electrons. If the particle kinetic energy in the beam frame is high in the comparison with the electron temperature, diffusion is insignificant and the particles are cooled. The method of electron cooling was originally suggested by A. M. Budker [7]. It was developed and studied then both theoretically and experimentally; an ample list of the references can be found in Ref. [8], for example.

Electron cooling can reduce the spread in all three components of beam momentum simultaneously. Its primary advantage over stochastic cooling is that the cooling effect is practically independent of antiproton beam intensity. Its greatest disadvantage is that the effect is very weak until the antiproton emittances are already close to the values wanted in the collider. Thus, the two processes can be seen as complementary rather than competitive. Electron cooling will prove very powerful in the Recycler as an add-on to the stochastic pre-cooling in the Antiproton Source and Recycler.

The ultimate goal is to realize a luminosity of  $0.5-1.0 \cdot 10^{33} \text{ cm}^{-2}\text{s}^{-1}$  in the Tevatron collider by supplying a larger flux of antiprotons. The conceptual design studies [9] demonstrate that this can be accomplished by providing longitudinal emittance cooling rates in the Recycler of 200 eV·s/h or higher (in conjunction with the transverse stochastic cooling). The primary technical problem is to generate a high-quality, monochromatic, dc, multi-MeV electron beam of 200 mA or greater.

The technical goal set in 1995 for an initial proof-of-principal demonstration using mostly existing equipment was to maintain a 200 mA beam for a period of one hour. The only technically feasible way to attain such high electron currents is through beam recirculation (energy recovery) [10]. This goal was achieved in 1998 by recirculating beam currents of 200 mA for periods of up to five hours without a single breakdown. Although the recirculation tests used a 1-1.5 MeV electron beam and the Recycler electron cooling system requires a 4.3 MeV beam, the demonstration is relevant because the increased energy does not involve fundamental changes in technology. Currently, the electron cooling group is building a full-scale, 4.3 MeV electron beam facility to complete the experimental R&D program and to prepare installation of the cooler in the Recycler ring.

#### *3.4.1.2 Project Scope*

Although electron cooling is well understood, the Recycler application represents a major step in beam energy, to 8 GeV from less than 1 GeV. The step is large enough that the high voltage generator, beam transport, and cooling region all require extension of the state of the art. Therefore, about two years (as of May, 2001) of research and development activity are likely to precede introduction of any electron cooling equipment into the Recycler.

The R & D phase of the project has the following goals:

1. optimized system parameter set (finished);
2. a reliable 4.3 MV electrostatic power supply (it is being commissioned as of May, 2001);

3. electron beam gun, collector and transport system to sustain a recirculating current of at least 0.5 A;
4. precise matching from discrete-element beam transport to continuous cooling region solenoid;
5. a 20 m cooling section with uniform axial magnetic field with precision such that p-bar transverse angles are  $\leq 10^{-4}$ ;
6. beam instrumentation and control to maintain alignment and equal mean velocity of electron and p-bar beams to precision  $\leq 10^{-4}$ , to measure beam angular spread and position, to determine neutralization, *etc.*

The laboratory developments are now being carried out in the downstream end of the Wideband Lab experimental area at Fermilab. There is sufficient space at Wideband to carry out the development work envisioned for the Recycler cooling project. The hardware aspects of the development program are treated in detail in Ref. [7]. The goal of the development program is cooling-system hardware ready for installation into the Recycler. The remainder of the work constitutes Accelerator Improvement Projects of moderate scale.

The basic tasks are:

1. Architectural design and civil construction of an enclosure for the high voltage generator and an interconnection tunnel to the MI tunnel for the electron beam transport. The work on this task has already started by Fermilab's FESS;
2. Installation of a Recycler lattice insertion for the cooling region. This task is almost finished. The Recycler lattice suitable for the electron cooling system exists. However, some p-bar trim magnets, diagnostics, and vacuum equipment will have to be installed upstream and downstream of the cooling section at the time of the cooler installation;
3. Installation of cooling section and electron beam transport channels;
4. Commissioning of the cooling system;

### **3.5 Rapid Antiproton Transfers**

#### ➤ Scope

The antiproton source lines serve to the following three major tasks: aiming 120 GeV protons coming out of the main injector to the antiproton production target, collection of 8 GeV antiprotons and sending them to the debuncher, and the transfer of cooled antiprotons from the accumulator to the main injector. The aim of the project is to minimize the emittance growth in the course of transfers and to maximize the collection of antiprotons coming out of the target.

#### ➤ Current status

Currently we experience multiple problems with the antiproton source transfer lines. They are: comparatively long setup time for beam transfers, the beam emittance growth related to dipole and quadrupole mismatches and jitter, and the beam scraping if the line is not well tuned. There are a few leading reasons for this misbehavior. First, the optics design is not sufficiently good. It has excessive values of  $\beta$ -functions and poor dispersion match, which yields increased sensitivity to errors and emittance growth. Second, poor knowledge of the real beam line focusing worsens envelope matches. Third, inaccurate field maps and inaccurate performing of hysteresis cycling reduces optics quality and reproducibility and leads to additional emittance growth. This problem is amplified by the fact that the same line is used for transport of 120 GeV protons and 8 GeV antiprotons.

#### ➤ Future Plans

The optics for focusing of protons on antiproton production target and for transfer of antiprotons from the accumulator to the main injector has been redesigned. That yielded more than a factor of two reduction of the maximum  $\beta$ -functions and a perfect match for beam envelopes and dispersion. That will decrease optics sensitivities to dipole and quadrupole errors and will increase free aperture of the line thus reducing the probability of scraping. This work also includes updates of field maps for quadrupoles, which should bring better coincidence between the design and real machine optics. To introduce this new optics we will need to perform reconnection of power supplies. That is planned for July 2001 shutdown.

Similar work is in progress for the collection of antiprotons from the target and their transfer to the debuncher. It is expected that understanding the problems and determining their cures will be formulated by the end of May 2001.

Further work includes optics measurements, their offline analysis and correction of the discrepancies between the design and real machine. Studies of the reproducibility of the optics are an important part of the plan. These include effective and fast optics measurements and their analysis and will require software for both the automation of the measurements and the analysis. Although these actions bring fast and significant improvements of beam transfers, at present we

do not have enough information about optics and therefore we cannot guaranty that they bring us to the “perfect” transfers. There is a probability that making the optics robust will require so much time and resources that it will be cheaper and faster to build a separate line for 8 GeV antiproton transfer (the AP5 line). The decision, about necessity of this new line, is anticipated by the end of 2001.

### **3.5.1 AP2 Line**

The AP2 beam line transports antiprotons, as part of a beam of secondary particles, from the production target and lens system to the Debuncher ring. Ideally, the aperture of the AP2 beam line should be the same as or larger than the Debuncher aperture. Some of the diagnostics of the AP2 beam line have recently been revived and used for some initial proton studies. Other diagnostics are in the process of being repaired and some are to be upgraded.

The current beam line BPM data acquisition is the original Z80 based system. An upgrade of the data acquisition part of the BPM system will improve precision and reliability. The existing AM/PM RF module will be used with a new sample and hold (being designed) and a commercial data acquisition. Currently, CDF experimenters are helping with the development of this system. A prototype system will be implemented this summer and used in parallel with the existing system.

There are 5 sets of collimators in the AP2 line. All have problems with the stepping motors and/or the read-back electronics. These should be fixed by the summer. The wire grids (SEMs) used for beam distribution measurements should all be in working order by summer; currently, a third of the detectors have either dead regions or do not work.

There is only one toroid at the end of AP2 line near the injection point to the Debuncher. Two 3 inch toroids had been removed since they were obvious aperture restrictions (AP2 beam pipe is nominally 6 inch). Larger toroids will be investigated.

No ‘local’ bumps are possible with the few existing dipole trim magnets in the AP2 beam line. At Debuncher injection, there are no trims to control the position. Several trims will be installed this summer; these trims will come from the defunct AP4 beam line. Further horizontal control at the AP2 ‘left bend’ will be implemented by a set of shunts.

Recently there has been work done at the AP2 injection point into the Debuncher: larger beam pipes and new components have been installed as well as re-orientation of components and beam pipe. As studies indicate, aperture fixes will be implemented when possible.

There is a study to match the AP2 into the Debuncher. The software tool being developed in tuning the AP2 lattice for the match will also be used to make lattice adjustments whenever the antiproton production target and lens system changes.

## **3.5.2 AP5 Line**

*3.5.2.1 Design*

*3.5.2.2 Civil*

*3.5.2.3 Technical Components*

## 3.6 Tevatron

### 3.6.1 Longitudinal Dynamics

#### 3.6.1.1 Scope of Project

In Run IIb, the number of proton bunches will be increased from 36 to 140 and the number of anti-proton bunches from 36 to 105. With this increase in current in the Tevatron, one of the things, which we will have to do, is to maintain the longitudinal stability of the bunches. Even now, at the start of Run IIa, we have already observed bunch oscillations, which persist for a very long time. Although we have not observed that these oscillations grow in time, they do dilute our longitudinal emittance unnecessarily. Therefore, it is important that we solve this problem in Run IIa before proceeding with any upgrade plans for Run IIb.

The scope of our project, therefore, is to understand the cause of these longitudinal oscillations and to provide remedies, which reduce these oscillations to a reasonable level. In particular for Run IIb, we want to anticipate the potential problems so that we can have good design parameters for longitudinal dampers.

In this paper, we will first discuss our observations in Run IIa and show our prescription for a cure. We will then show a basic longitudinal damper design for Run IIb with discussion about some of its problems.

#### 3.6.1.2 Current Status

At the beginning of Run IIa, it has been observed that when the Tevatron was injected with uncoalesced bunches which were spaced a bucket apart, the bunches were oscillating longitudinally seemingly without correlation. Furthermore, these oscillations persisted for an extremely long time (>1 hour), without any signs of decay.

In order to remove the phenomena of coupled bunch modes from clouding our understanding, we used one coalesced bunch to understand the problem. **Figure 3-18** shows a mountain range plot of a single coalesced bunch dipole (and quadrupole) oscillating. Each trace of the plot represents 20 turns in the Tevatron. An interesting observation developed that we could actually reduce the longitudinal oscillations by changing the injection phase. This can be seen in **Figure 3-19**. This then gave us a clue to the cause of the longitudinal oscillations.

We focused in on the first turn bunches from the Main Injector into the Tevatron and found to our surprise that the bunches did not have constant phase with respect to the Tevatron RF. **Figure 3-20** and **Figure 3-21** show the uncoalesced bunches at different spots of the batch. The markers were fixed at 58 ns but clearly the four bunches within between the markers were at different places. In fact the error is about 2 ns between the first picture and the second picture. This meant that the Main Injector injected bunches with random phases into the Tevatron and any injection phase tuning which we could do could only fix the average phase error.

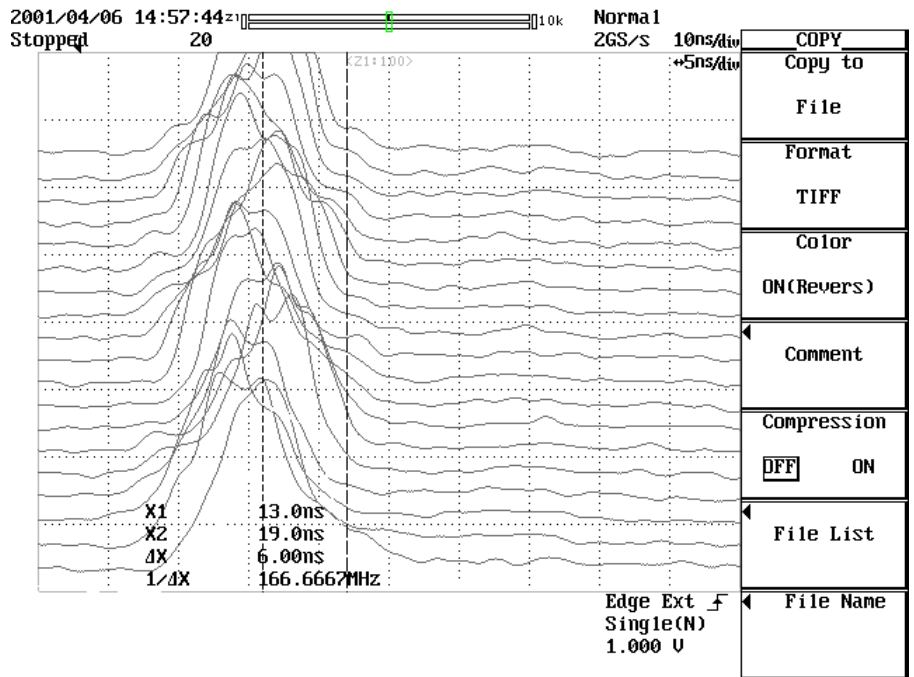


**Figure 3-18** This figure shows the longitudinal oscillations of a coalesced bunch when the injection phase between the Main Injector and the Tevatron is not matched.

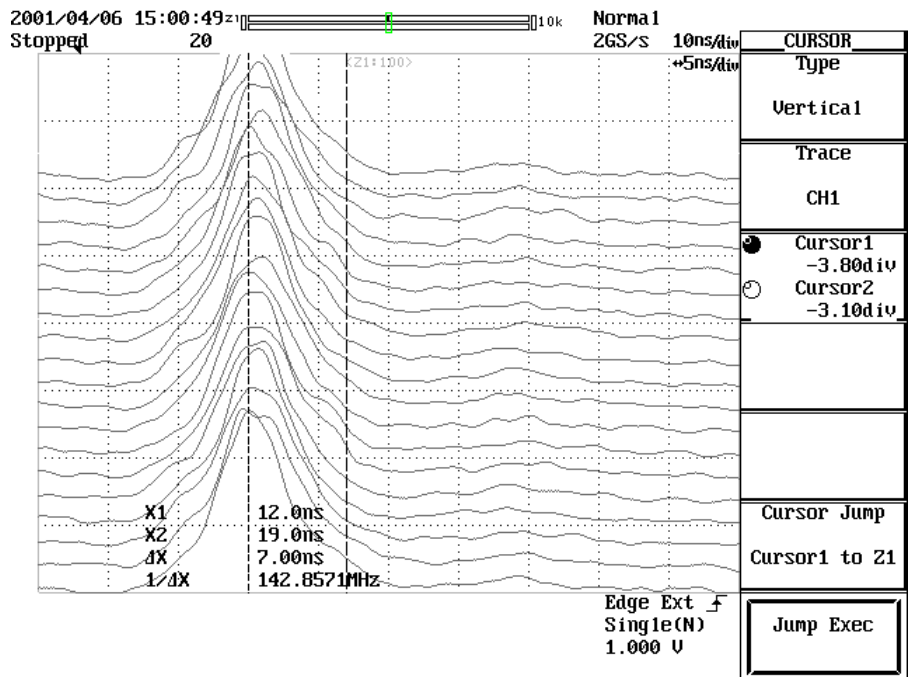


**Figure 3-19** The longitudinal oscillations are much smaller when the injection phase between the Main Injector and Tevatron are tuned to match.

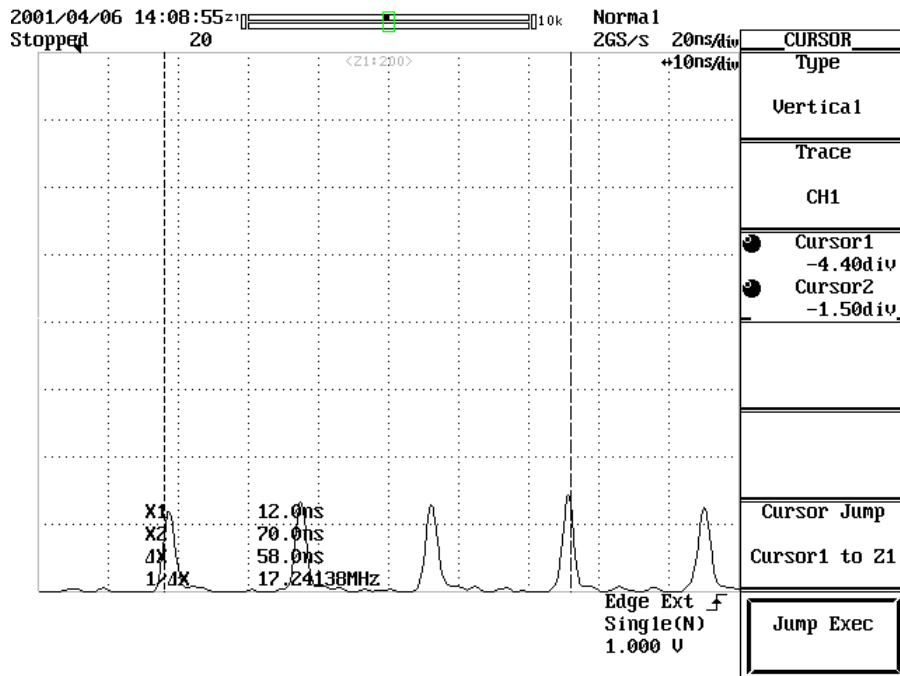


**Figure 3-20**

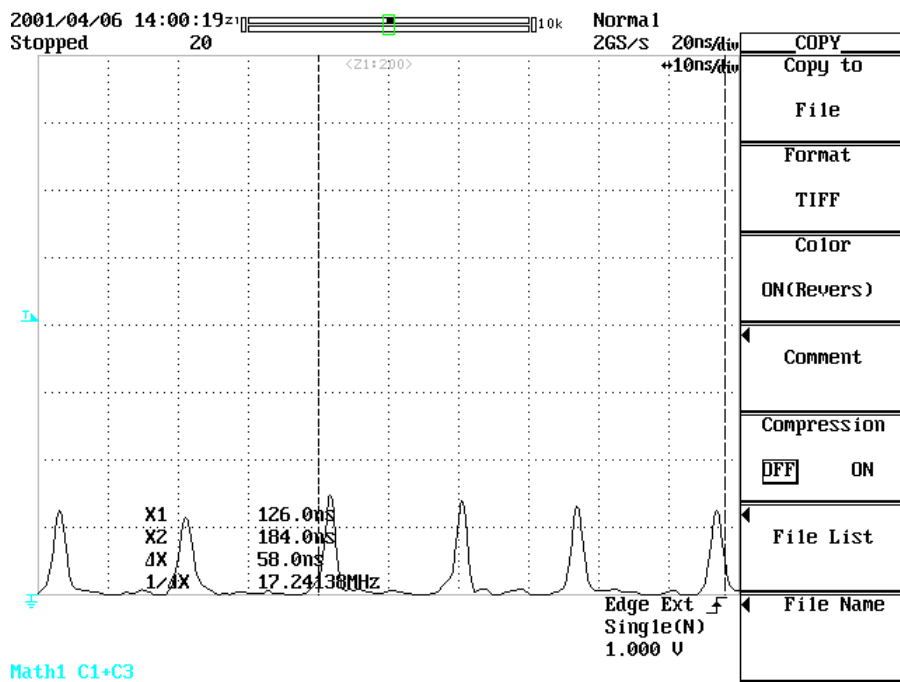


**Figure 3-21** These two figures show the injection phase errors in the same uncoalesced bunch train. The distance between the markers is 58ns in both figures but clearly the bunches are at different injection phases.

### 3.6.1.3 Future Plans

We plan to build a mode 0 and mode 1 dipole damper shown in **Figure 3-23**. The idea is to see if by damping out these coupled bunch modes, the single bunch oscillations themselves will be sufficiently damped for Run IIa.

If this design is insufficient to damp out the oscillations, we will upgrade to a bunch by bunch damper shown in **Figure 3-24**. Due to the closeness of the bunches, this design will require an upgrade to the phase shifter because it only has a 1 MHz bandwidth. Furthermore, because the frequency response of the cavity at its fundamental is very sharp, this will imply that phase shifting will require more power than we presently have.

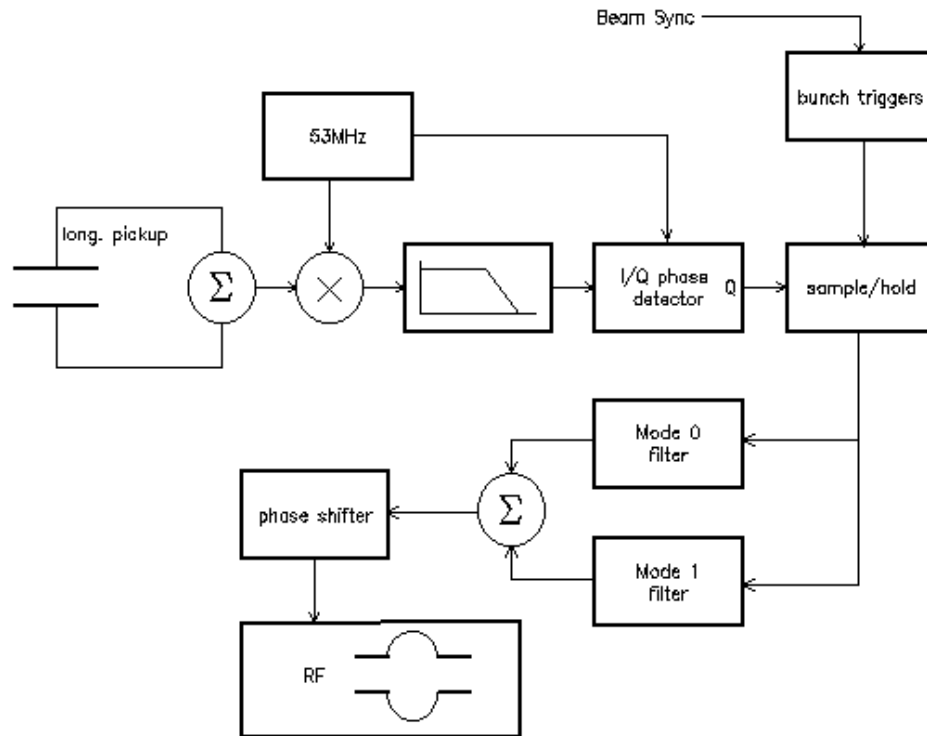


**Figure 3-23** Longitudinal dampers which will damp out modes 0, and 1 coupled bunch dipole modes.

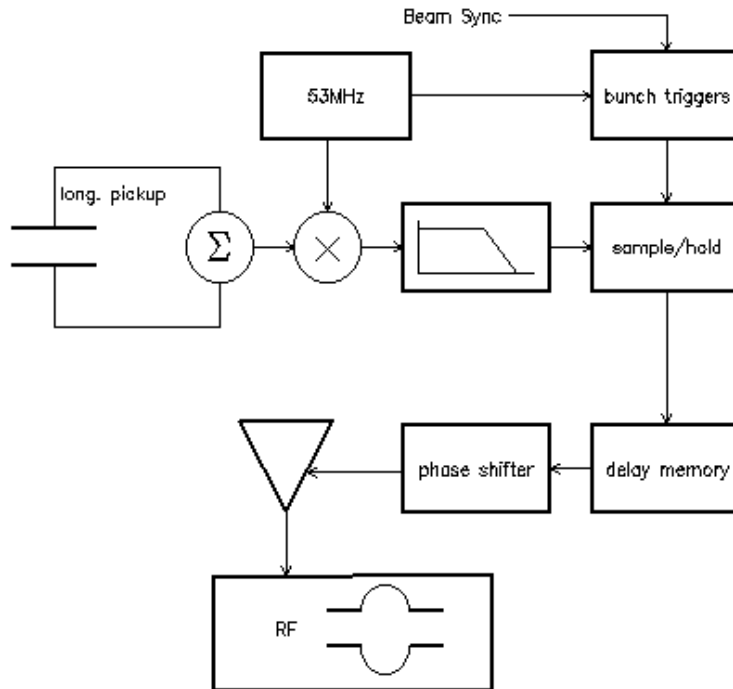


**Figure 3-24** Upgraded bunch by bunch longitudinal dampers.

### 3.6.2 Beam-Beam Tune Shift Compensation

#### 3.6.2.1 Scope

The beam-beam interaction in the Tevatron collider sets limits on bunch intensity and luminosity. These limits are caused by a tune spread in each bunch which is mostly due to head-on collisions, but there is also a bunch-to-bunch tune spread due to parasitic collisions in multibunch operation. It has been proposed to compensate these effects with use of a counter-traveling low-energy high current electron beams – see, e.g. *V.Shiltsev, et.al, Phys.Rev. ST-AB, 071001 (July 1999)*.

Beam-beam interaction between protons and antiprotons takes place at the two head-on interaction points (IPs, located at B0 and D0 sectors), as well as at numerous parasitic crossings where the beam orbits are separated by about dozen rms beam sizes. Since the proton beam intensity is several times the antiproton intensity, the beam-beam effects are more severe for antiprotons. It is to be noted that the design value of the total tune shift for antiprotons is about the maximum experimentally achieved value for proton colliders  $dQ \sim 0.025$ . The "footprint area" of the pbar beam with such a tune shift is large enough to also cause an increase of particle losses due to higher order lattice resonances.

In order to achieve sufficient beam-beam separation away from the IPs, a crossing angle of about 200 microradian between proton and antiproton orbits at the main interaction points can be used. Besides the geometrical luminosity reduction, the crossing angle may lead to synchrotron coupling, additional resonances, beam blow-up and luminosity degradation although the maximum tune shift becomes smaller with the angle.

The Tevatron beam injection requires some gaps in the bunch train that results in the so-called “PACMAN effect” -- bunch-to-bunch variation of the betatron tunes due to long-range beam-beam interactions. The effect depends on the orbit separation around the ring and is most visible for bunches close to the gaps. For example, during Run IIb with 140 proton and 121 antiproton colliding bunches the tune spread within each bunch and the bunch-to-bunch tune spread are both about 0.008. During Run II with 36 bunches in each beam, the bunch-to-bunch spread is expected to be about 0.007, while the single bunch tune spread will be about 0.018. These tune spreads are expected to be a problem for the collider operation if uncorrected.

Two electron beam setups for compensation of the beam-beam effects in the Tevatron (TEL-Tevatron Electron Lens) are to be installed away from the proton-antiproton interaction points at B0 and D0. They provide the electron beams which collide with the antiproton beam. The electron beam is to be created on an electron gun cathode, transported through the interaction region in a strong solenoidal magnetic field, and absorbed in the collector. In principle, since the electron charge is opposite to the proton charge, the electromagnetic force on antiprotons, due to the proton beam, can be compensated by the electron beam. The proton beam has to be separated from the electron and antiproton beams in the device.

There are two implementations of the proposal:

1) an “electron lens” with modulated current to provide different linear defocusing forces for different antiproton bunches in order to equalize their betatron frequencies (further referred as *linear compensation*); and 2) an “electron compressor”, that is a nonlinear DC electron lens which compensates (on average) the nonlinear focusing due to the proton beam – *nonlinear compensation*. The latter has a potential for *crossing angle elimination*.

It is hard to give exact quantitative estimates on the collider luminosity improvement due to the BBC, but based on a simple relation between peak luminosity and the maximum beam-beam parameter  $L \propto \xi$  one can say that in the Run IIb the *linear* Beam-Beam Compensation may potentially lead to some 50% luminosity increase, the *nonlinear compensation* to a 2-3-fold increase, and the *crossing angle elimination* may add some 40% by allowing collisions without the crossing angle.

### 3.6.2.2 Status

Fermilab Beams Division BBC (Beam-Beam Compensation) Project group is currently focused on the *linear BBC*. For that one TEL has been designed, built, tested, installed in the Tevatron Sector F48 and commissioned by March 1, 2001. Because of the larger horizontal beta function  $\beta_x=101\text{m} \gg \beta_y=29\text{m}$  at that location, the first TEL can shift mostly horizontal tune of the Tevatron beams. It is anticipated that the second TEL to be built and installed at the Sector A10

where  $\beta_y=172\text{m} \gg \beta_x=56\text{m}$  will shift mostly vertical betatron tune. TEL general view and main parameters are presented below.

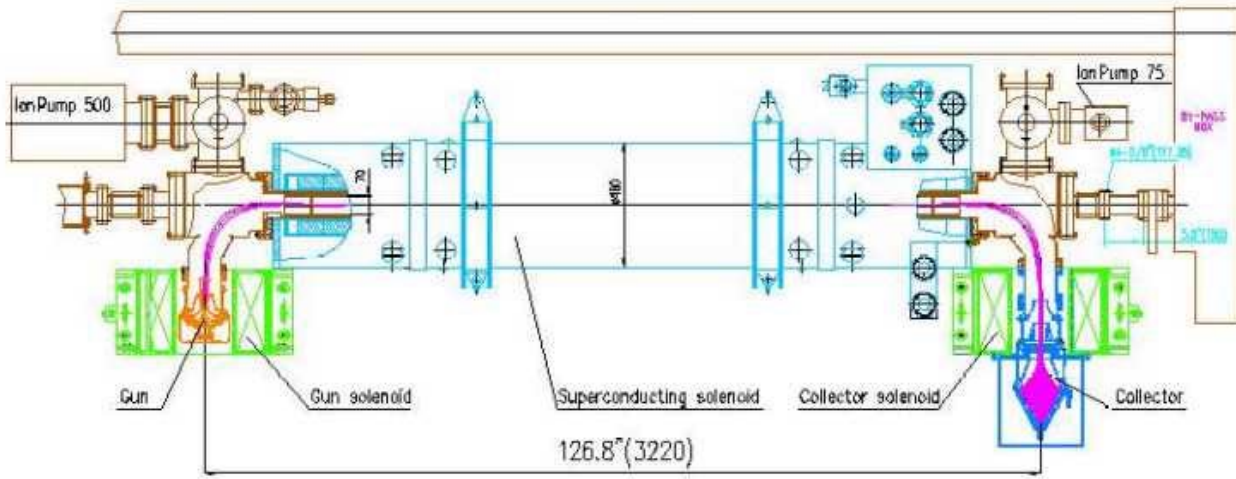


**Table 3-1**

Beam diameter in the gun/main solenoid	10/3	mm
Beam energy, max	15	kV
Beam current, pulsed, max	3.5	A
Effective interaction length	2.1	m
Magnetic field on cathode/main solenoid	0-4.2 / 0-65 (default 3.8/35)	kG
Current stability, dJ/J peak-to-peak	0.02	%
Electron current pulse width, total	~800	ns

In March-April 2001, the TEL operated in a single bunch regime with 47.7 kHz electron pulse repetition rate. Maximum horizontal tuneshift achieved with 980 GeV protons (6 shift of studies) is about  $dQ_x=+0.0071$  with 980 GeV protons, while vertical tune shift is about 4 times less – all in a good agreement with theoretical expectations. Among other achievements: a) a decent proton beam lifetime exceeding 20 hrs is obtained with maximum electron current; b) it's demonstrated that electron beam separated by 5 mm from the proton beam – default regime for the BBC, as the electron beam will collide with pbars – does not affect the proton beam (infinite lifetime); c) in general, having TEL magnets on and/or electron beam not interacting with Tevatron beams does produce no significant effects on the Tevatron beams (no significant changes in orbits, tunes, coupling, chromaticity, dispersion, lifetime, impedance, etc.).

### 3.6.2.3 Further Studies and Plans

Further plans of the BBC project in FY01, FY02 include beam studies and building the second TEL.

Beam studies will be devoted to: a) operation with 980 GeV antiprotons; b) investigation of the p(pbar) lifetime dependence on e-beam steering, current, size and shape, magnetic field, current and position stability, p(pbar) size; c) understanding of the ion accumulation process and relevant effects, clearing/storing of ions; d) measurement of the p(pbar) emittance evolution under impact of the TEL; e) attempting improvement dynamics of a single pbar bunch by the only existing TEL; f) studies of non-linear effects under operational conditions similar to those required by the *non-linear BBC*; g) observation of “strong head-tail” instability at smaller main solenoid magnetic field. In parallel, we will continue hardware improvement, e.g., electron gun, electron and p(pbar) beam-position monitors, electron beam diagnostics, power supplies stabilization, higher power HV modulators.

Building the second TEL will require: a) studies of the bending section magnetic field optimization and potential design changes in positioning gun and collector solenoid magnets; b) fabrication of the magnetic system and quench protection system for SC magnets; c) building electron gun, collector, diagnostics and vacuum system; d) design and fabrication of a faster HV modulator for Run IIb operation; e) assembly and test of the TEL in E4R building; f) preparation work at A10 sector, including radiation shielding for SC magnets and cryogenics infrastructure; g) installation and commissioning of the second TEL; h) modification of the control system.

## 4. Resources, Cost, Schedule

### 4.1 Project Goals

The project schedule was developed to accommodate the luminosity schedule shown in Table 4-1. Such a schedule is illustrated in terms of initial store luminosity in **Figure 4-1** and in terms of integrated luminosity in Figure 4-2.

**Table 4-1** Schedule Goal

Fiscal Year	Luminosity 1.00E+31	Months of Ops.	Shut- downs (months)	Cycle Time Factor	Integrated Luminosity (Year)	Integrated Luminosity (Total)	Money Spent %	Comments
FY01	3	8	4	1	0.2	0.2	12	Slightly in excess of best previous performance
FY02	8	10	2	1	0.8	1.0	36	Install 132 nS equipment.
FY03	12	8	4	1	1.0	2.0	60	Go to 132nS. Shut down for Electron Cooling
FY04	20	11	1	0.8	1.8	3.8	81	Initiate NUMI with 20% impact
FY05	40	8	4	0.8	2.6	6.3	100	Shutdown for Run IIb Silicon & C-0 IR
FY06	50	11	1	0.8	4.4	10.7	100	
FY07	50	10	2	0.8	4.0	14.7	100	

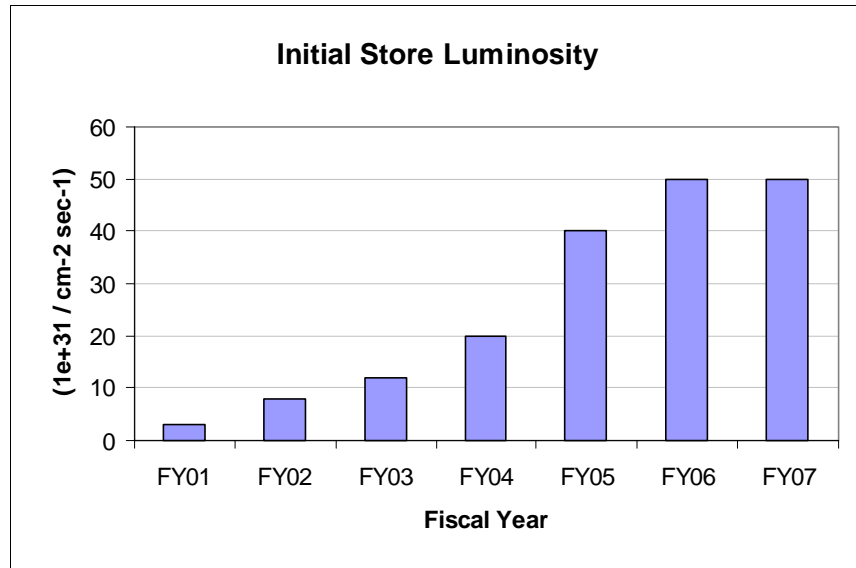


**Figure 4-1** Initial Luminosity

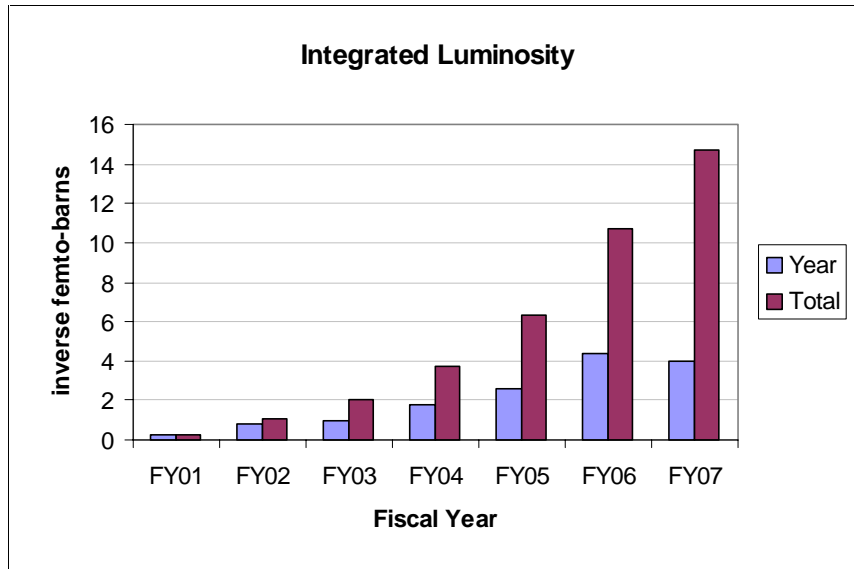


**Figure 4-2** Integrated Luminosity

One notes that the goal of  $15 \text{ fb}^{-1}$  is indeed achievable if an initial luminosity of  $5 \cdot 10^{32} \text{ cm}^{-2} \text{ sec}^{-1}$  can be achieved.

It is interesting to compare the evolution of the luminosity in terms of percentage of goal in comparison to the expenditure of resources. This is indicated in **Figure 4-3**.

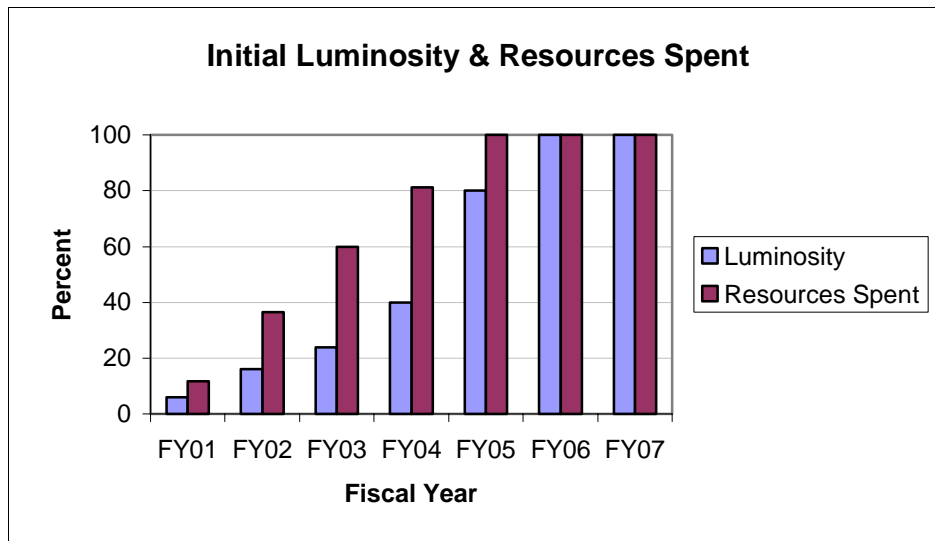


**Figure 4-3** Comparison of resources spent versus percentage of luminosity goal achieved as a function of time.

## 4.2 Project Costs by Sub-Project

The project has been developed thus far as a series of sub-projects which are shown grouped by primary machine area or equivalently by primary unit within the Beams Division organization.

The costs as a function of financial year, including both Materials and Services and Salaries, are summarized in Table 4-2.

**Table 4-2** *Project and Sub-project Costs as a function of Financial Year*

	FY01	FY02	FY03	FY04	FY05	Run IIb	Start	Operational
	Total	Total	Total	Total	Total	Total	Date	Date
<b>PS</b>	<b>249</b>	<b>367</b>	<b>389</b>	<b>231</b>	<b>0</b>	<b>1235</b>	<b>Mar - FY01</b>	<b>Mar - FY04</b>
Linac	149	167	139	231	0	<b>685</b>	Mar - FY01	Jun - FY04
Ion Source R&D	149	167	139	231	0	<b>685</b>	Mar - FY01	Jun - FY04
Linac RFQ	0	0	0	0	0	<b>0</b>	-	-
Booster	100	200	250	0	0	<b>550</b>	Apr - FY01	Jul - FY03
Booster Cavities	0	0	0	0	0	<b>0</b>	-	-
Ramped Correctors	75	100	125	0	0	<b>300</b>	Feb - FY01	Jul - FY03
Longitudinal Dampers	0	0	0	0	0	<b>0</b>	-	-
Transverse Dampers	0	0	0	0	0	<b>0</b>	-	-
Cogging	25	100	125	0	0	<b>250</b>	Oct - FY02	Jul - FY03
<b>MI</b>	<b>77</b>	<b>693</b>	<b>0</b>	<b>0</b>	<b>0</b>	<b>770</b>	<b>Oct - FY02</b>	<b>Aug - FY02</b>
RF	77	693	0	0	0	<b>770</b>	Oct - FY02	Aug - FY02
Slip Stacking	77	693	0	0	0	<b>770</b>	Oct - FY02	Aug - FY02
Low Level	34	306	0	0	0	<b>340</b>	Oct - FY02	Aug - FY02
Beam Loading Compens	43	387	0	0	0	<b>430</b>	Sept - FY01	Aug - FY02
RF Power Upgrade	0	0	0	0	0	<b>0</b>	-	-
<b>RR</b>	<b>2384</b>	<b>5637</b>	<b>5960</b>	<b>600</b>	<b>0</b>	<b>14580</b>	<b>May - FY01</b>	<b>Aug - FY03</b>
Electron Cooling	2050	2700	4200	600	0	<b>9550</b>	Mar - FY01	Aug - FY03
AP5 line	334	2937	1760	0	0	<b>5030</b>	Oct - FY02	Jun - FY03
Design	110	115	125	0	0	<b>350</b>	Jan - FY01	Jun - FY03
Civil	211	1409	810	0	0	<b>2430</b>	Oct - FY02	Jun - FY03
Technical Components	13	1413	825	0	0	<b>2250</b>	Nov - FY02	Jun - FY03

	FY01	FY02	FY03	FY04	FY05	Run llb	Start	Operational
	Total	Total	Total	Total	Total	Total	Date	Date
<b>Pbar</b>	<b>329</b>	<b>673</b>	<b>1128</b>	<b>5824</b>	<b>5987</b>	<b>13940</b>	<b>Feb - FY03</b>	<b>Jul - FY05</b>
Target Station	97	291	291	1291	1000	<b>2970</b>	Jun - FY02	Jun - FY05
Solid Lens R&D	97	291	291	1291	1000	<b>2970</b>	Jun - FY02	Jun - FY05
Liquid Lens R&D	0	0	0	0	0	<b>0</b>	-	-
Beam Sweeping	0	0	0	0	0	<b>0</b>	-	-
Debuncher	197	197	197	2368	2567	<b>5525</b>	Jul - FY03	Jul - FY05
Aperture	197	197	197	1543	1742	<b>3875</b>	Sept - FY02	Jul - FY05
BPM System	62	62	62	310	224	<b>720</b>	Nov - FY02	Jun - FY05
Moveable Quads	135	135	135	808	538	<b>1750</b>	Jan - FY02	Jun - FY05
Dipole Beam Pipe	0	0	0	425	980	<b>1405</b>	Jan - FY04	Aug - FY05
DRF1-1	0	0	0	0	0	<b>0</b>	-	-
Lattice Upgrades	0	0	0	825	825	<b>1650</b>	Dec - FY04	Jul - FY05
Coupling Correction	0	0	0	350	350	<b>700</b>	Dec - FY04	Jul - FY05
Resonance Correction	0	0	0	350	350	<b>700</b>	Dec - FY04	Jul - FY05
Gamma - t ramp	0	0	0	75	75	<b>150</b>	Dec - FY04	Jul - FY05
Dispersion Correction	0	0	0	50	50	<b>100</b>	Dec - FY04	Jul - FY05
Accumulator	0	0	0	1400	2270	<b>3670</b>	Jan - FY04	Aug - FY05
StackTail Betatron Coolin	0	0	0	450	740	<b>1190</b>	Jan - FY04	Aug - FY05
Core Transverse Cooling	0	0	0	450	740	<b>1190</b>	Jan - FY04	Aug - FY05
StackTail Pickups	0	0	0	500	790	<b>1290</b>	Jan - FY04	Aug - FY05
Beam Lines	35	185	640	765	150	<b>1775</b>	Jul - FY02	Sept - FY04
Beam Position System	0	0	465	155	0	<b>620</b>	Nov - FY03	May - FY04
AP2 line	35	185	175	610	150	<b>1155</b>	Mar - FY02	Dec - FY05
Aperture	35	185	175	610	150	<b>1155</b>	Mar - FY02	Dec - FY05
Left Bends	0	10	0	610	150	<b>770</b>	Nov - FY04	Mar - FY05
Correctors	35	175	175	0	0	<b>385</b>	Oct - FY02	Jul - FY03
Chromatic Correction	0	0	0	0	0	<b>0</b>	-	-
AP1 Line	0	0	0	0	0	<b>0</b>	-	-
EPB dipole replacemen	0	0	0	0	0	<b>0</b>	-	-
F17 Cmagnet Replacen	0	0	0	0	0	<b>0</b>	-	-
<b>TEV</b>	<b>1000</b>	<b>1110</b>	<b>555</b>	<b>648</b>	<b>463</b>	<b>3775</b>	<b>Feb - FY01</b>	<b>Dec - FY05</b>
Tune Shift Compensation	1000	1110	555	648	463	<b>3775</b>	Feb - FY01	Dec - FY05
Beam Loading Compensati	0	0	0	0	0	<b>0</b>	-	-
Longitudinal Dampers	0	0	0	0	0	<b>0</b>	-	-
<b>Run llb Total</b>	<b>4038</b>	<b>8479</b>	<b>8032</b>	<b>7302</b>	<b>6449</b>	<b>34300</b>	<b>Aug - FY01</b>	<b>Mar - FY05</b>

It can be seen from **Table 4-2** that there are a number of sub-projects, for which there is currently no funding plan or for which it has been necessary to defer the start of the project because of lack of resources. In a sense the decision as to which sub-projects fall into this category is a part of the plan.

**Liquid Lithium Lens** This project is based on an R&D program underway at BINP. There is not enough funding available in the current budget guidance to continue this project.

**AP2 and Debuncher Aperture Increase** This project should start in FY2002. However, there is not enough funding available in the current budget guidance to start this project until FY2004.

**Accumulator Stack Tail Cooling** This project should start in FY2003. However, there is not enough funding available in the current budget guidance to start this project until FY2004.

**Tevatron Beam Loading Compensation** There is not enough funding available in the current budget guidance to do this project.

**Tevatron Longitudinal Dampers** There is not enough funding available in the current budget guidance to do this project.

**Linac Front End Upgrade** There is not enough funding available in the current budget guidance to do this project.

**Booster RF Cavities** There is not enough funding available in the current budget guidance to do this project.

### 4.3 Project Effort

We have some estimates of the effort needed to execute the project. This is broken down by effort type and by FY in Table 4-3.

**Table 4-3** Effort by year, organizational unit and effort type.

	FY01																
	Total	M&S	Labor	Phys	EE	Engr	Draft	Tech	ME	Engr	Draft	Tech	RF	Engr	Draft	Tech	CP
PS	249	43	2.1	1.7	0.0	0.0	0.0	0.0	0.1	0.0	0.0	0.0	0.2	0.1	0.0	0.1	0.1
MI	77	20	0.6	0.0	0.0	0.0	0.0	0.0	0.0	0.0	0.0	0.0	0.5	0.3	0.0	0.2	0.1
RR	2384	1050	13.3	5.1	2.0	1.0	0.0	1.0	6.2	2.1	2.1	2.0	0.0	0.0	0.0	0.0	0.0
Pbar	329	145	1.8	0.2	0.1	0.0	0.0	0.1	1.3	0.3	0.3	0.7	0.2	0.1	0.0	0.1	0.1
TEV	1000	500	5.0	2.0	1.0	0.5	0.0	0.5	2.0	0.5	0.5	1.0	0.0	0.0	0.0	0.0	0.0
<b>Run IIb T</b>	<b>4038</b>	<b>1758</b>	<b>22.8</b>														

	FY02																
	Total	M&S	Labor	Phys	EE	Engr	Draft	Tech	ME	Engr	Draft	Tech	RF	Engr	Draft	Tech	CP
PS	367	67	3.0	1.3	0.0	0.0	0.0	0.0	0.5	0.1	0.2	0.2	0.2	0.8	0.4	0.0	0.4
MI	693	180	5.1	0.2	0.0	0.0	0.0	0.0	0.0	0.0	0.0	0.0	0.0	4.5	2.7	0.0	1.8
RR	5637	3500	21.4	6.6	2.0	1.0	0.0	1.0	12.8	4.9	4.9	3.0	0.0	0.0	0.0	0.0	0.0
Pbar	673	285	3.9	0.7	0.3	0.0	0.0	0.3	2.5	0.6	0.7	1.3	0.2	0.1	0.0	0.1	0.2
TEV	1110	600	5.1	1.2	1.8	0.6	0.0	1.2	2.1	0.6	0.3	1.2	0.0	0.0	0.0	0.0	0.0
<b>Run IIb T</b>	<b>8479</b>	<b>4632</b>	<b>38.5</b>														

	FY03																
	Total	M&S	Labor	Phys	EE	Engr	Draft	Tech	ME	Engr	Draft	Tech	RF	Engr	Draft	Tech	CP
PS	389	73	3.2	1.3	0.0	0.0	0.0	0.0	0.4	0.1	0.2	0.2	1.0	0.5	0.0	0.5	0.5
MI	0	0	0.0	0.0	0.0	0.0	0.0	0.0	0.0	0.0	0.0	0.0	0.0	0.0	0.0	0.0	0.0
RR	5960	4000	19.6	4.6	2.0	1.0	0.0	1.0	12.0	4.0	4.0	4.0	0.0	0.0	0.0	0.0	1.0
Pbar	1128	510	6.2	1.0	0.3	0.0	0.0	0.3	2.5	0.6	0.7	1.3	1.7	0.9	0.0	0.9	0.7
TEV	555	300	2.6	0.6	0.9	0.3	0.0	0.6	1.1	0.3	0.2	0.6	0.0	0.0	0.0	0.0	0.0
<b>Run IIb T</b>	<b>8032</b>	<b>4883</b>	<b>31.5</b>														

	FY04																
	Total	M&S	Labor	Phys	EE	Engr	Draft	Tech	ME	Engr	Draft	Tech	RF	Engr	Draft	Tech	CP
PS	231	38	1.9	1.3	0.0	0.0	0.0	0.0	0.7	0.1	0.3	0.3	0.0	0.0	0.0	0.0	0.0
MI	0	0	0.0	0.0	0.0	0.0	0.0	0.0	0.0	0.0	0.0	0.0	0.0	0.0	0.0	0.0	0.0
RR	600	250	3.5	1.5	0.5	0.5	0.0	0.0	1.0	0.3	0.5	0.3	0.0	0.0	0.0	0.0	0.5
Pbar	5824	2890	29.3	5.5	0.1	0.1	0.0	0.0	16.9	4.8	4.2	7.9	6.0	3.0	0.0	3.0	0.8
TEV	648	350	3.0	1.2	0.6	0.2	0.0	0.3	0.7	0.2	0.2	0.3	0.0	0.0	0.0	0.0	0.5
<b>Run IIb T</b>	<b>7302</b>	<b>3528</b>	<b>37.7</b>														

	FY05																
	Total	M&S	Labor	Phys	EE	Engr	Draft	Tech	ME	Engr	Draft	Tech	RF	Engr	Draft	Tech	CP
PS	0	0.0	0.0	0.0	0.0	0.0	0.0	0.0	0.0	0.0	0.0	0.0	0.0	0.0	0.0	0.0	0.0
MI	0	0.0	0.0	0.0	0.0	0.0	0.0	0.0	0.0	0.0	0.0	0.0	0.0	0.0	0.0	0.0	0.0
RR	0	0.0	0.0	0.0	0.0	0.0	0.0	0.0	0.0	0.0	0.0	0.0	0.0	0.0	0.0	0.0	0.0
Pbar	5987	2985.0	30.0	4.5	0.1	0.1	0.0	0.0	18.6	4.4	3.7	10.5	5.7	1.7	0.0	4.0	1.2
TEV	463	250.0	2.1	1.0	0.3	0.1	0.0	0.1	0.4	0.1	0.1	0.1	0.0	0.0	0.0	0.0	0.5
<b>Run IIb T</b>	<b>6449</b>	<b>3235.0</b>	<b>32.1</b>														

Expressed in terms of cost, these numbers, broken down by year and organizational unit, are shown in **Table 4-4**.

**Table 4-4** Effort Cost by organizational unit and year

	FY01	FY02	FY03	FY04	FY05	Total
PS	205.5	299.5	316.25	193.75	0	1015
MI	57	513	0	0	0	570
RR	1333.5	2136.5	1960	350	0	5780
Pbar	184	388	618	2933.5	3001.5	7125
TEV	500	510	255	297.5	212.5	1775
Total	2280	3847	3149.25	3774.75	3214	16265

The two projections of this table are shown graphically in **Figure 4-4** and **Figure 4-1**.

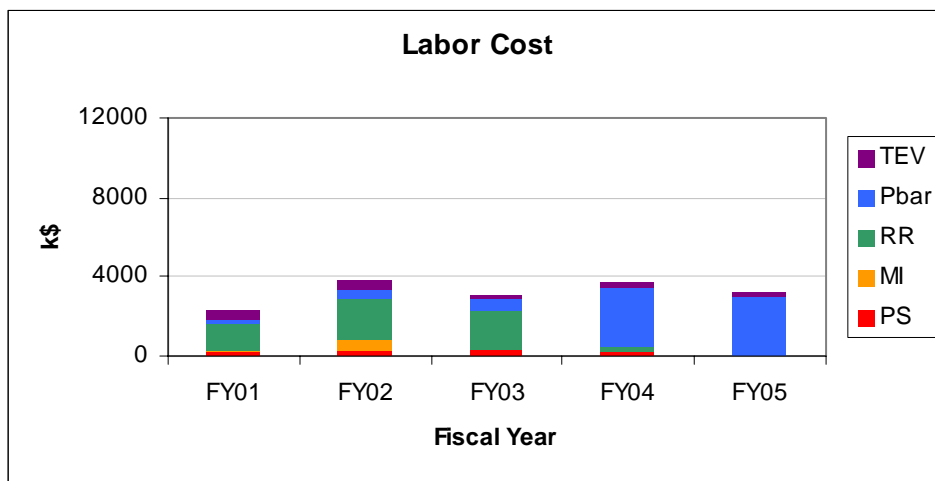


**Figure 4-4** Labor Cost by Fiscal Year.

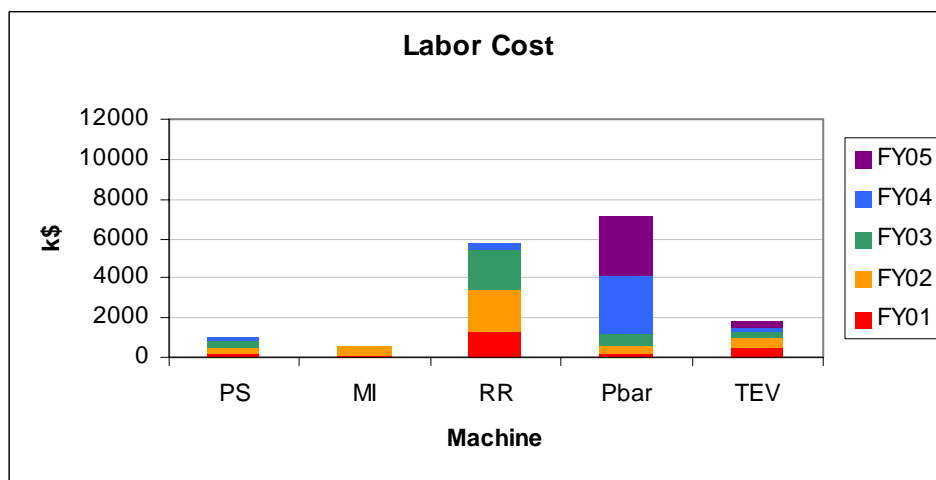


**Figure 4-5** Labor Cost by Fiscal Year

#### 4.4 Project Materials and Service Costs

Materials and services cost, broken down by year and organizational unit, are shown in **Table 4-5**

**Table 4-5** Materials and Services costs by organizational unit and year

	FY01	FY02	FY03	FY04	FY05	Total
PS	43	67	72.5	37.5	0	220
MI	20	180	0	0	0	200
RR	1050	3500	4000	250	0	8800
Pbar	145	285	510	2890	2985	6815
TEV	500	600	300	350	250	2000
<b>Total</b>	<b>1758</b>	<b>4632</b>	<b>4882.5</b>	<b>3527.5</b>	<b>3235</b>	<b>18035</b>

The two projections of this table are shown graphically in **Figure 4-6** and **Figure 4-7**.

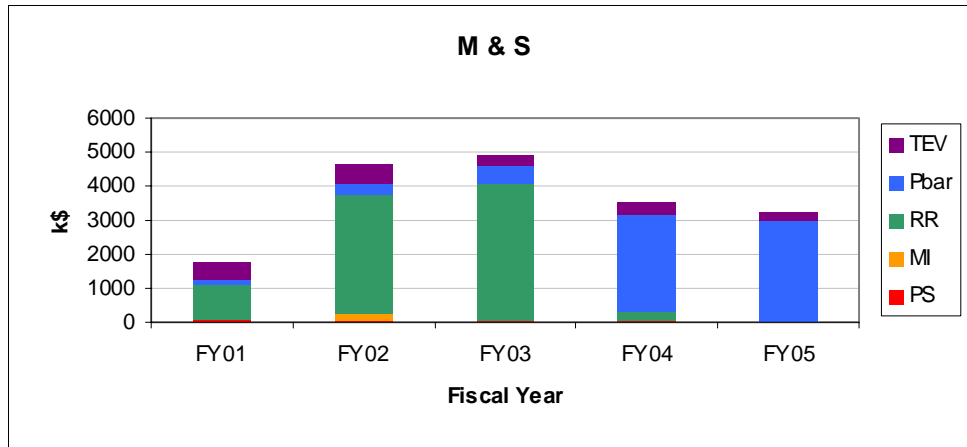


**Figure 4-6** Materials and Services Costs by Financial Year

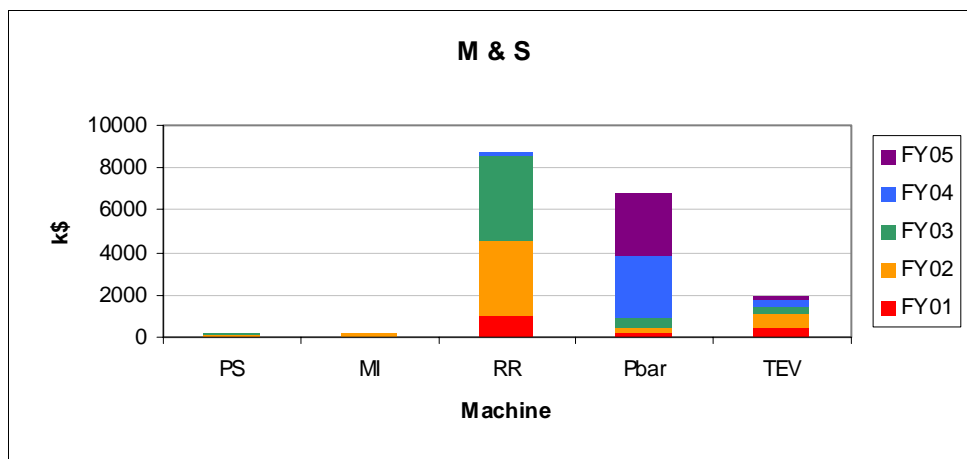


**Figure 4-7** Materials and Services Costs by Organizational Unit

#### 4.5 Project Total Cost

Materials and services cost, broken down by year and organizational unit, are shown in **Table 4-6**.

**Table 4-6** Project Total Costs by Organizational Unit and Financial Year

	FY01	FY02	FY03	FY04	FY05	Total
PS	249	367	389	231	0	1235
MI	77	693	0	0	0	770
RR	2384	5637	5960	600	0	14580
Pbar	329	673	1128	5824	5987	13940
TEV	1000	1110	555	648	463	3775
Total	4038	8479	8032	7302	6449	34300

The two projections of this table are shown graphically in **Figure 4-8** and **Figure 4-9**.

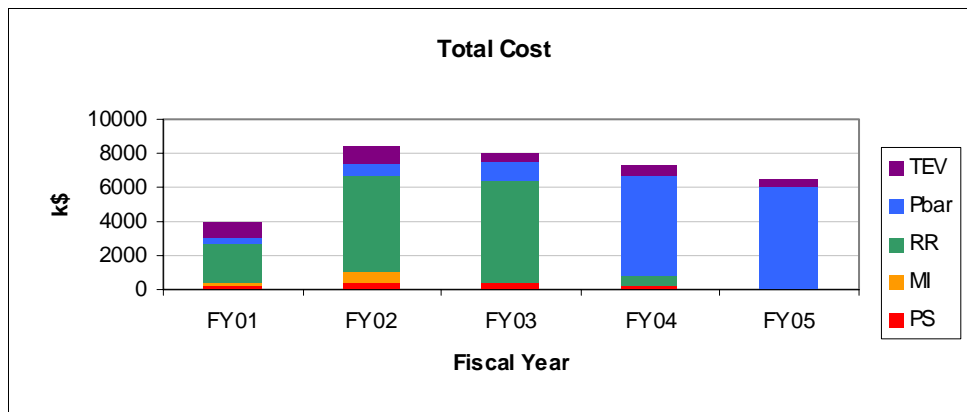


**Figure 4-8** Total cost as function of Fiscal Year.

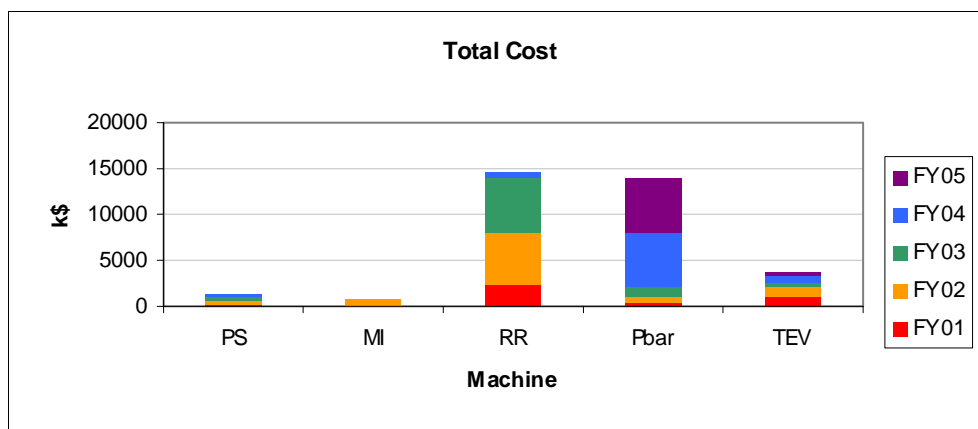


**Figure 4-9** Total Cost as function of organizational unit.



## 5. Summary

Over the past year, considerable progress has been made towards defining a practical and responsive plan for the improvements to the Fermilab accelerator complex for Run IIB.

Some projects have been discarded or at least put to one side for the moment. Some projects have been included with the knowledge that further refinement of their scope is necessary.

At the present time the estimates of needed resources are dominated by top-down estimates.

We feel that we are in a position to consolidate and attack some projects and to entertain discussion of corrections to others. In particular we must try and ensure that the project becomes robust with respect to its goals.

## 6. References

1. The TeV33 Committee Report, February 1996.
2. Report on Plans of the Beams Division for Tev33, 1997, unpublished.
3. Run II Handbook,
4. Proton Driver Study, Fermilab-TM-2136, December 2000.
5. D. B. Cline et al., "Intermediate Energy Electron Cooling for Antiproton Sources Using a Pelletron Accelerator", IEEE Trans. Nucl. Sci., NS-30, no. 4 (1983), p2370.
6. Delbert J. Larson, "Intermediate Energy Electron Cooling for Antiproton Sources", PhD dissertation, U. Wisconsin, Madison WI (1986).
7. A. M. Budker, Atomnaja Energija, 22 (5), p246 (1967).
8. I. N. Meshkov, Phys. Part. Nucl., 25 (6), p631 (1994).
9. A. Burov, *et al.*, "Design of Antiproton Medium Energy Electron Cooling at Fermilab", NIM A 441 (2000), 234.
10. A.C. Crawford, S. Nagaitsev, A. Sharapa, and A. Shemyakin, "Successful MeV-range electron beam recirculation", in Proc. of EPAC-98 (Stockholm, Sweden, June 22-26, 1998).
11. J. MacLachlan (editor), "Prospectus for an electron cooling system for the Recycler", Fermilab-TM-2061, <http://www-lib.fnal.gov/archive/1998/tm/TM-2061.html>